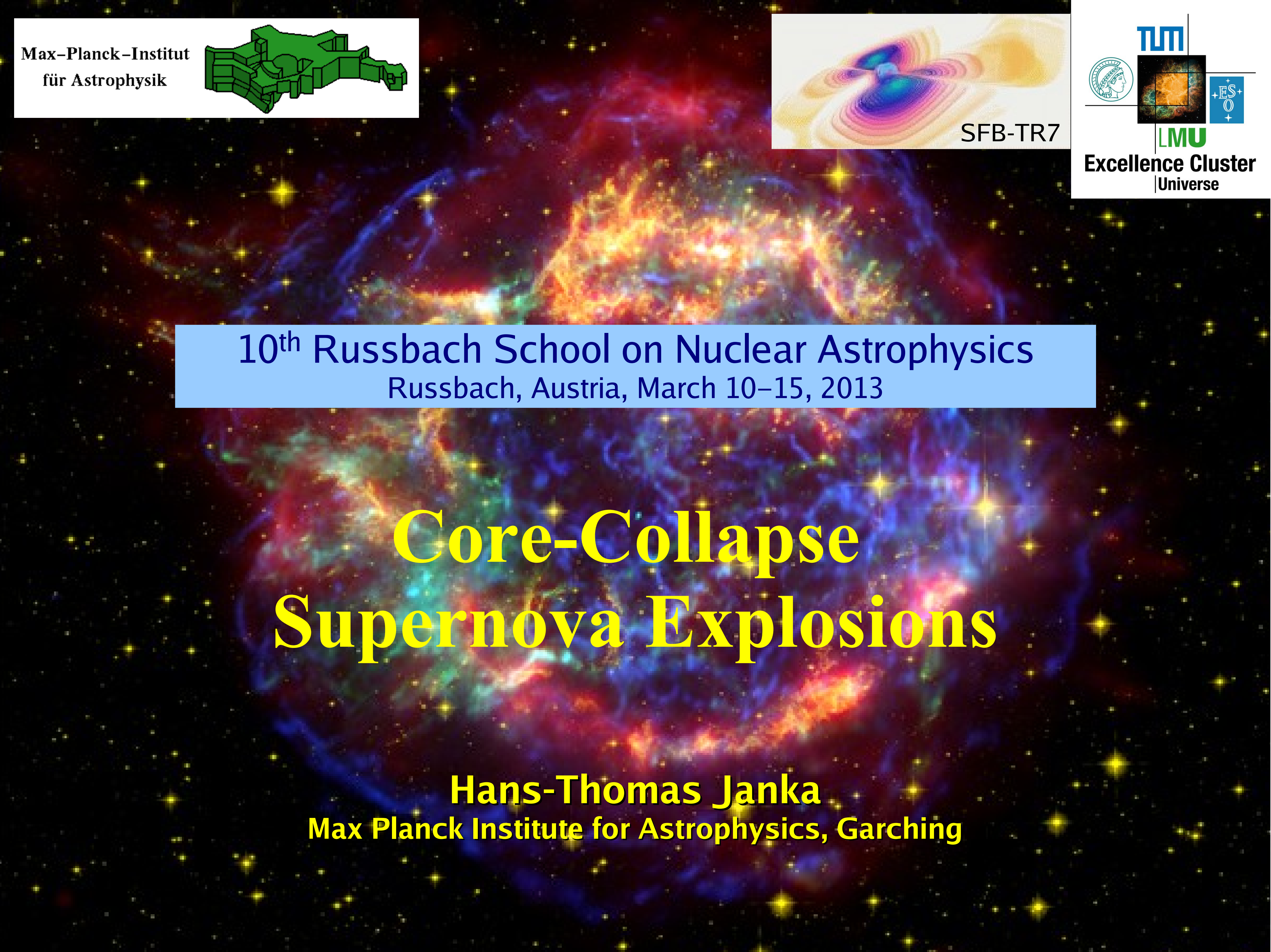

Max-Planck-Institut für Astrophysik

SFB-TR7

TUM LMU Excellence Cluster Universe

10th Russbach School on Nuclear Astrophysics

Russbach, Austria, March 10-15, 2013

Core-Collapse Supernova Explosions

Hans-Thomas Janka

Max Planck Institute for Astrophysics, Garching

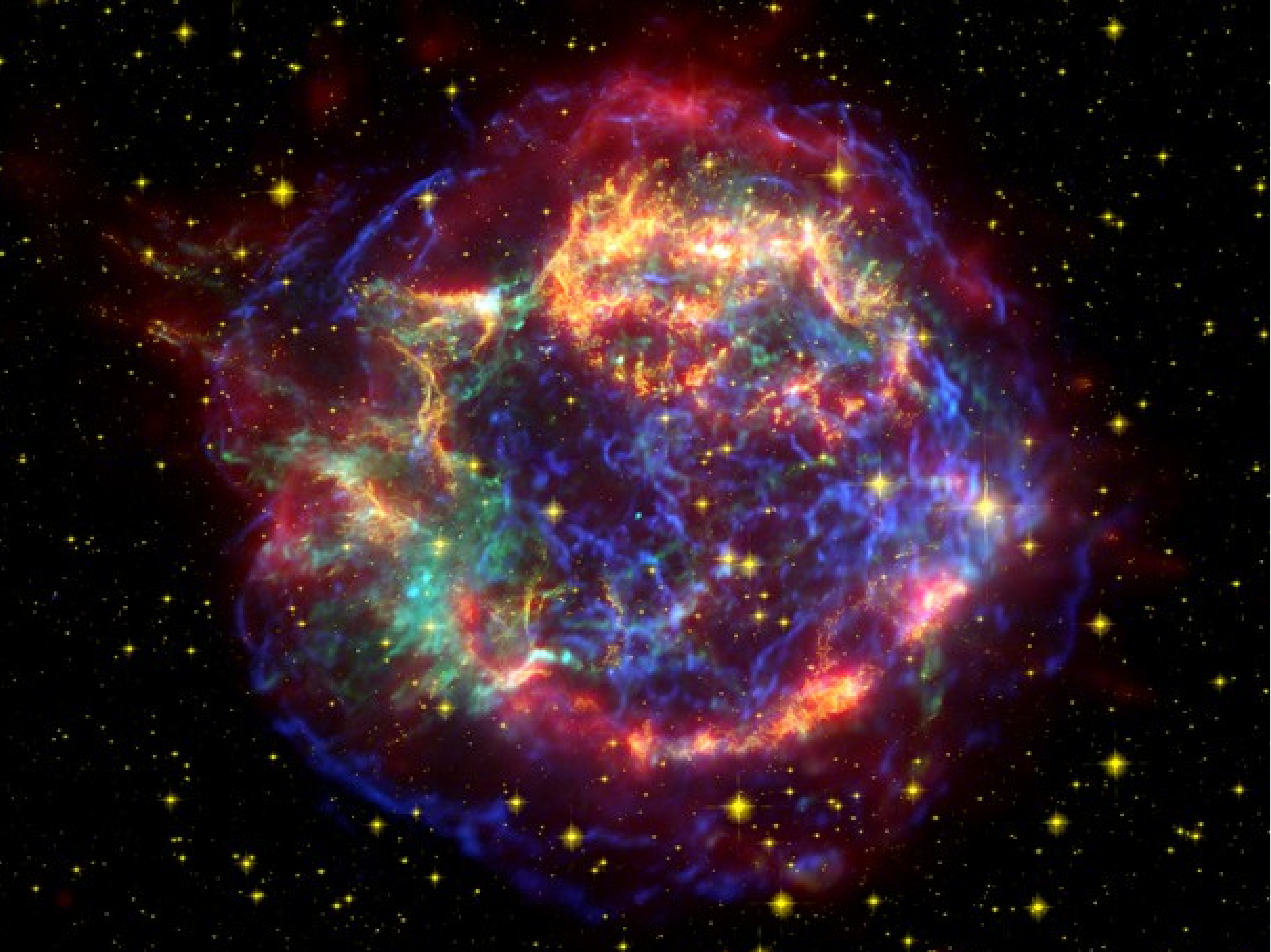

Outline

- Introduction to core-collapse supernova dynamics
- The neutrino-driven mechanism
- Status of self-consistent models in two dimensions
- The dimension conundrum: How does 3D differ from 2D?

Final Stages of Massive Star Evolution

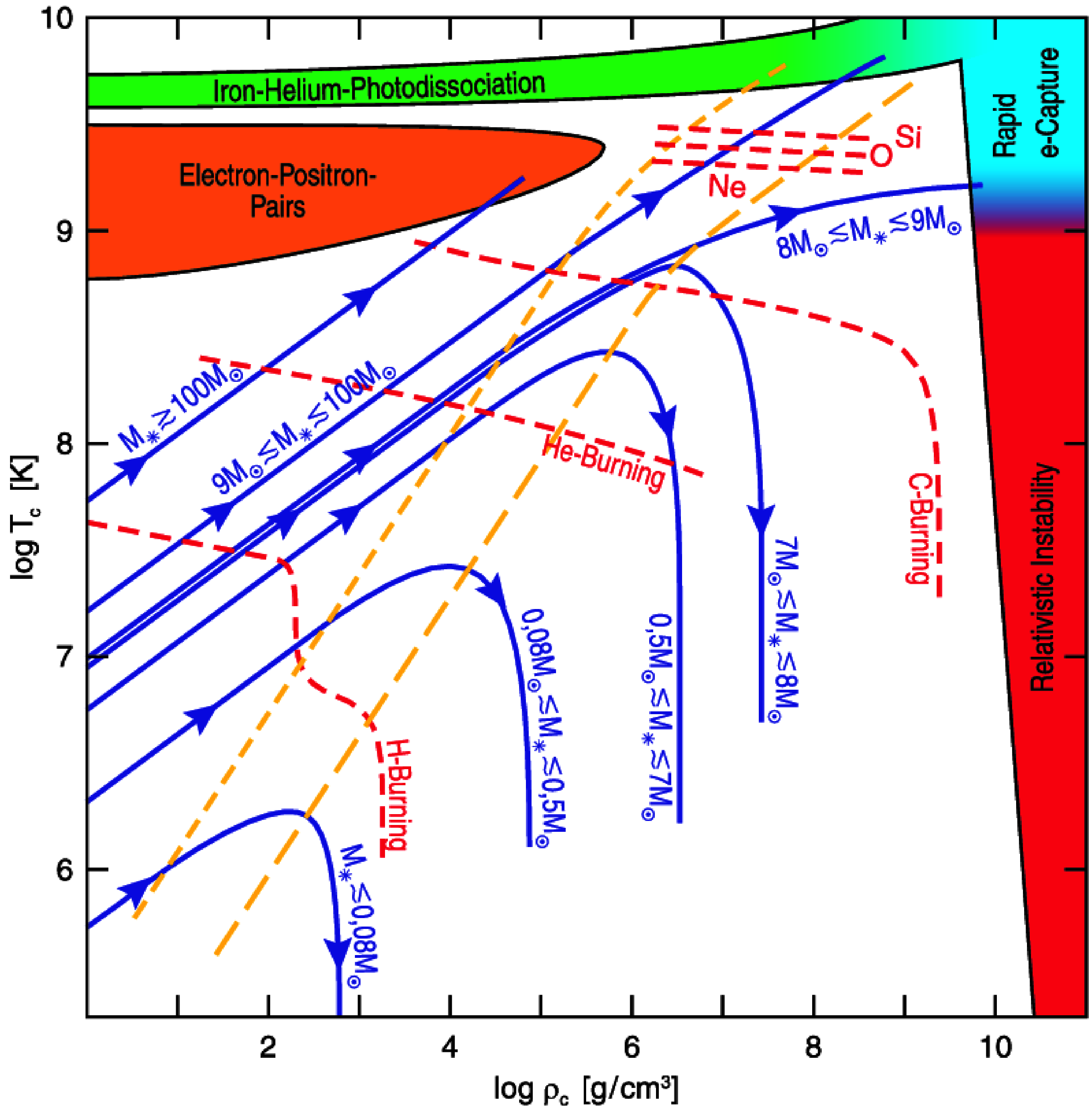

Janka, ARNPS 62, 407 (2002)

Stellar Core Collapse and Explosion

Evolved massive star prior to its collapse:

Star develops onion-shell structure in sequence of nuclear burning stages over millions of years

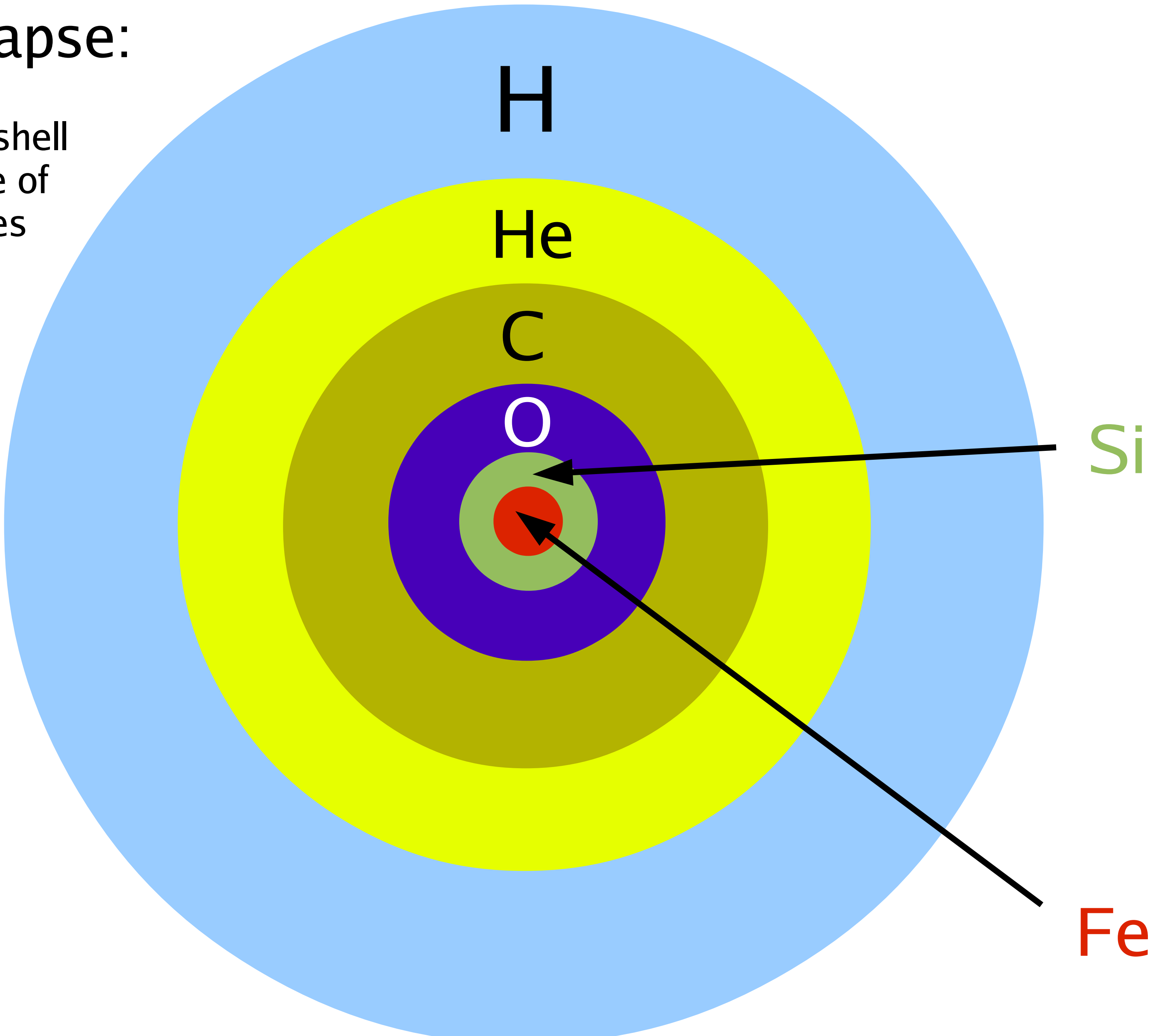

(layers not drawn to scale)

Evolved massive star prior to its collapse:

Star develops onion-shell structure in sequence of nuclear burning stages over millions of years

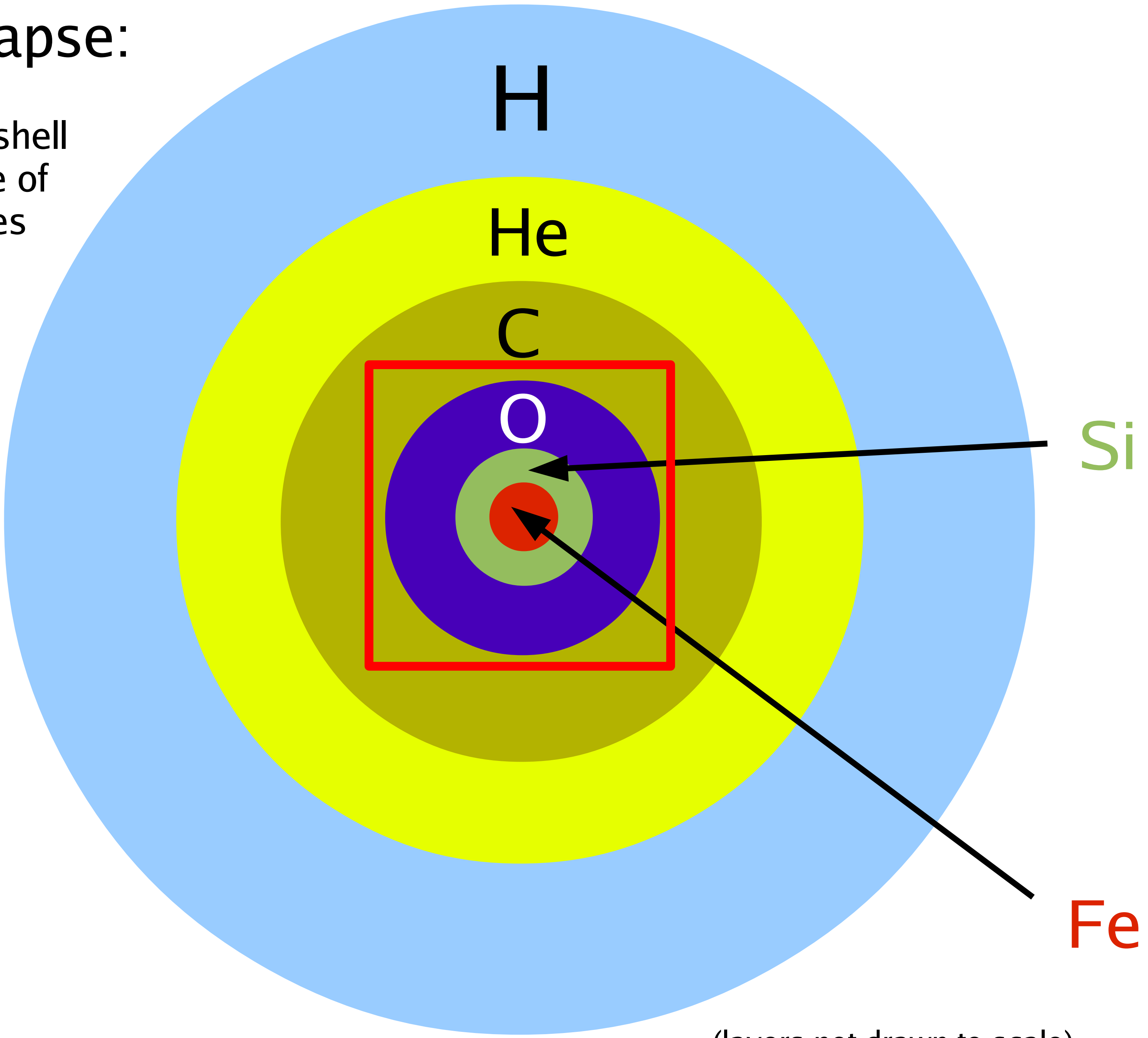

(layers not drawn to scale)

Gravitational instability of the stellar core:

Stellar iron core begins collapse when it reaches a mass near the critical Chandrasekhar mass limit

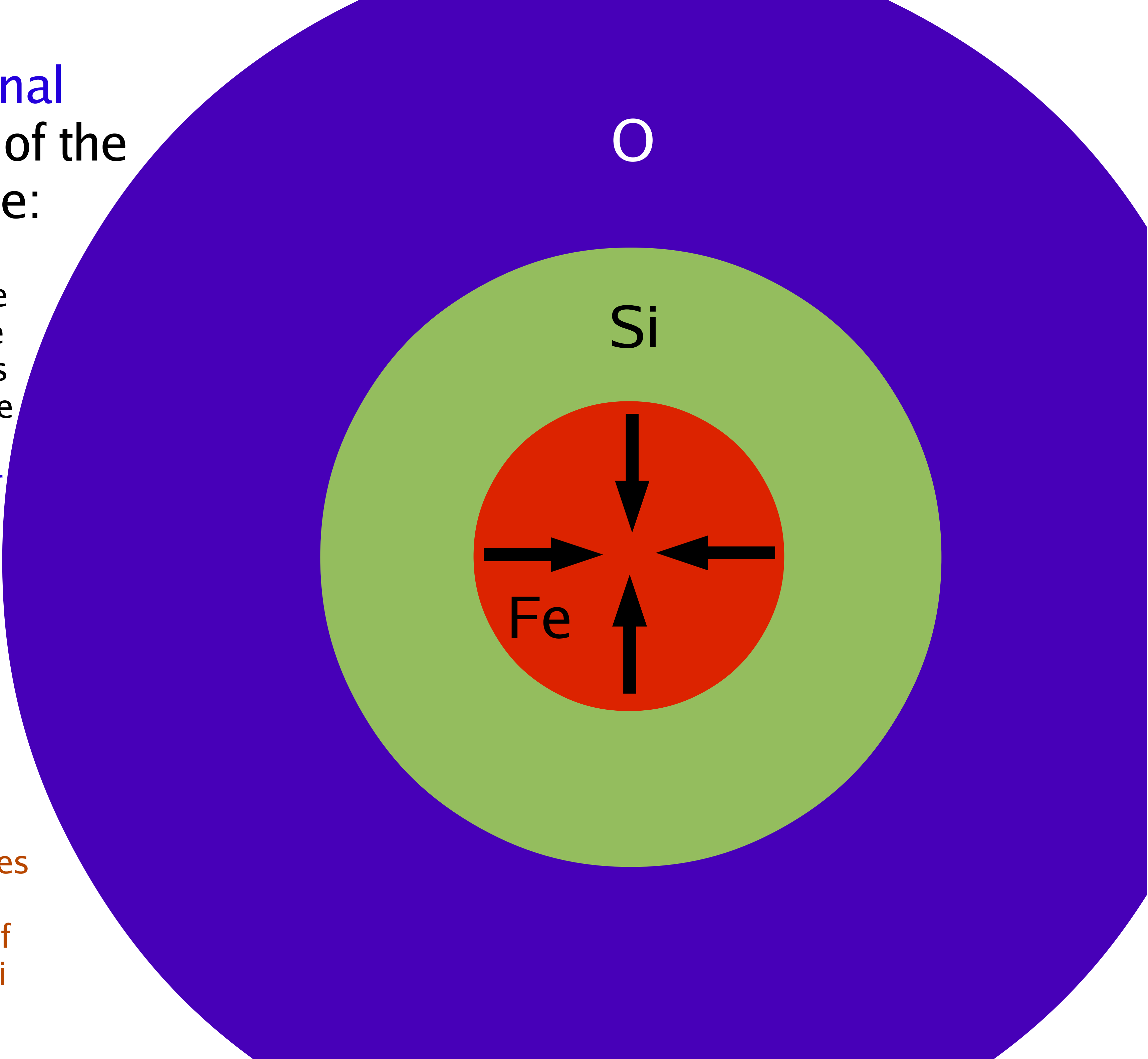

Collapse becomes dynamical because of electron captures and photo-disintegration of Fe-group nuclei

Core bounce at nuclear density:

Inner core bounces when nuclear matter density is reached and incompressibility increases

Shock wave forms

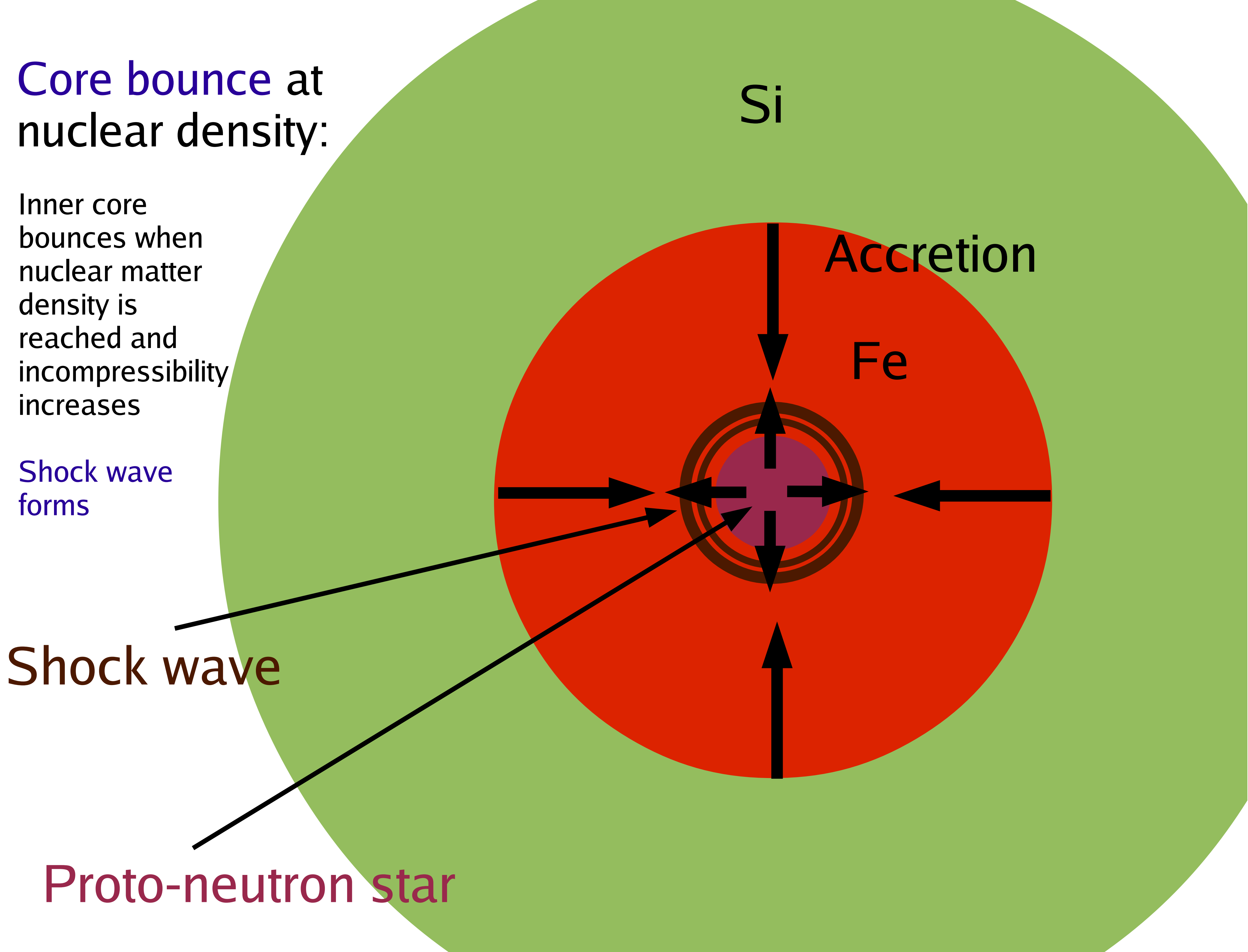

Shock stagnation:

Shock wave loses huge amounts of energy by photo-disintegration of Fe-group nuclei.

Shock stagnates still inside Fe-core

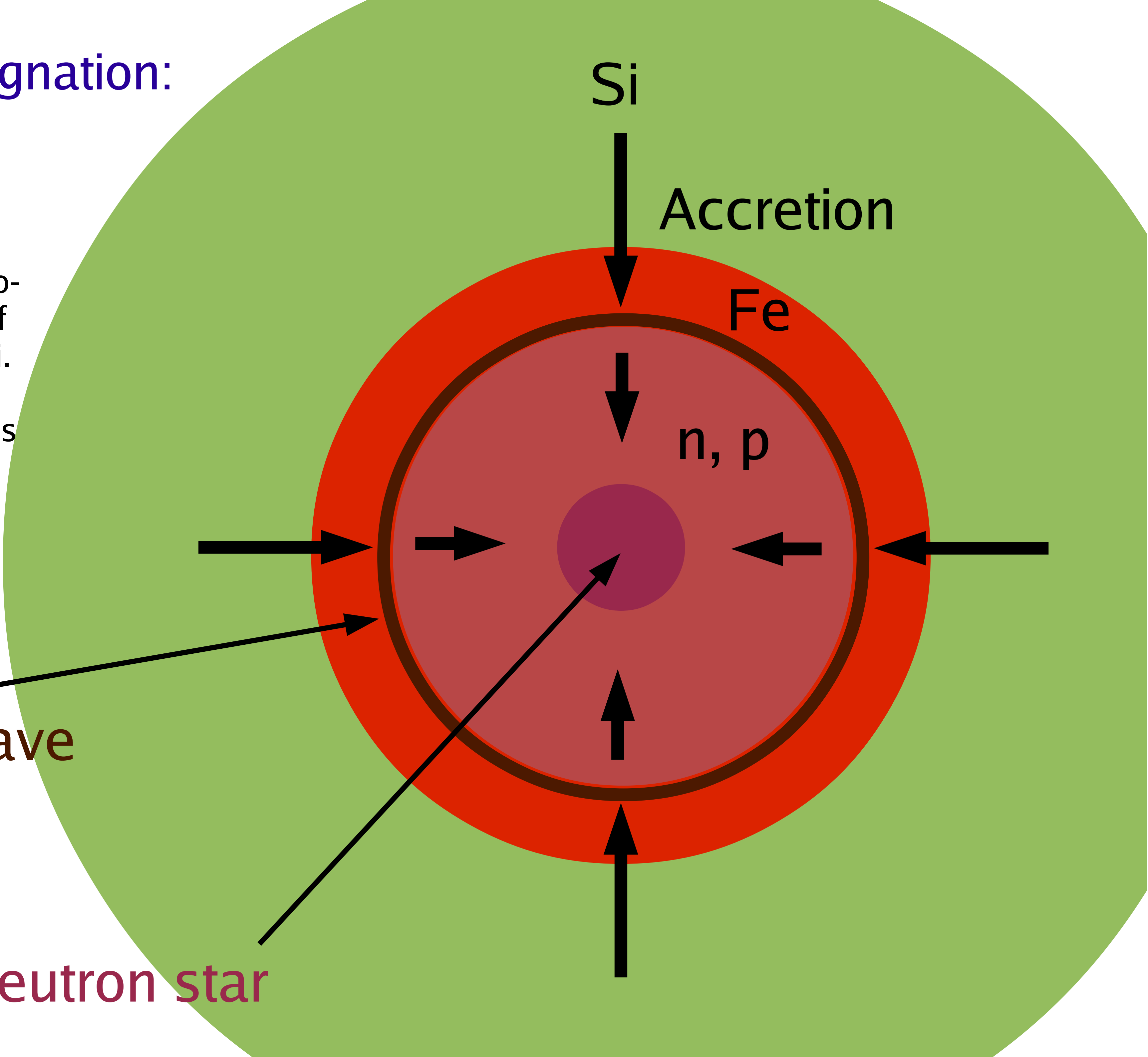

Explosion Mechanism by Neutrino Heating

Shock “revival”:

Stalled shock wave must receive energy to start reexpansion against ram pressure of infalling stellar core.

Shock can receive fresh energy from neutrinos!

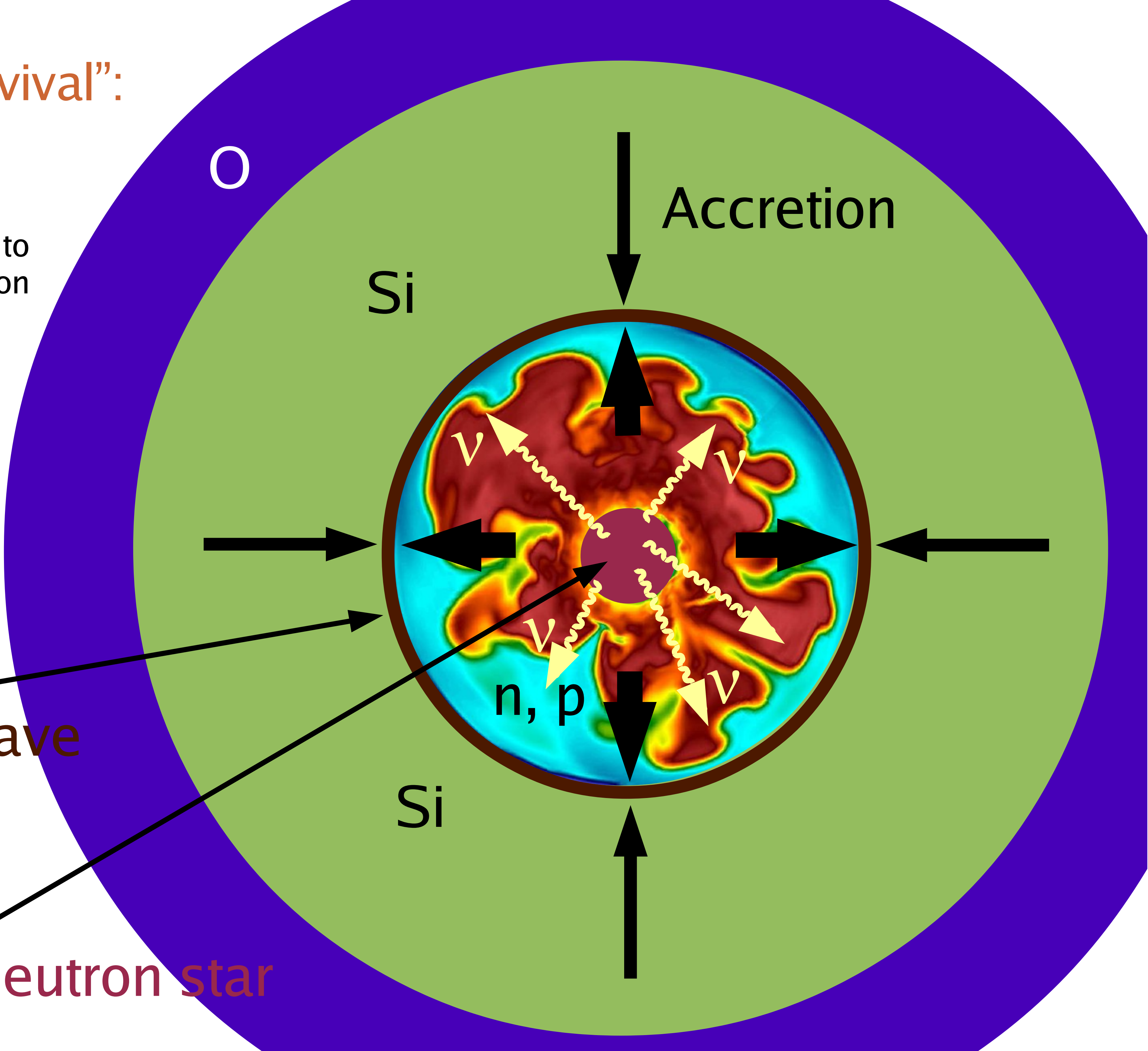

Explosion:

Shock wave expands into outer stellar layers, heats and ejects them.

Creation of radioactive nickel in shock-heated Si-layer.

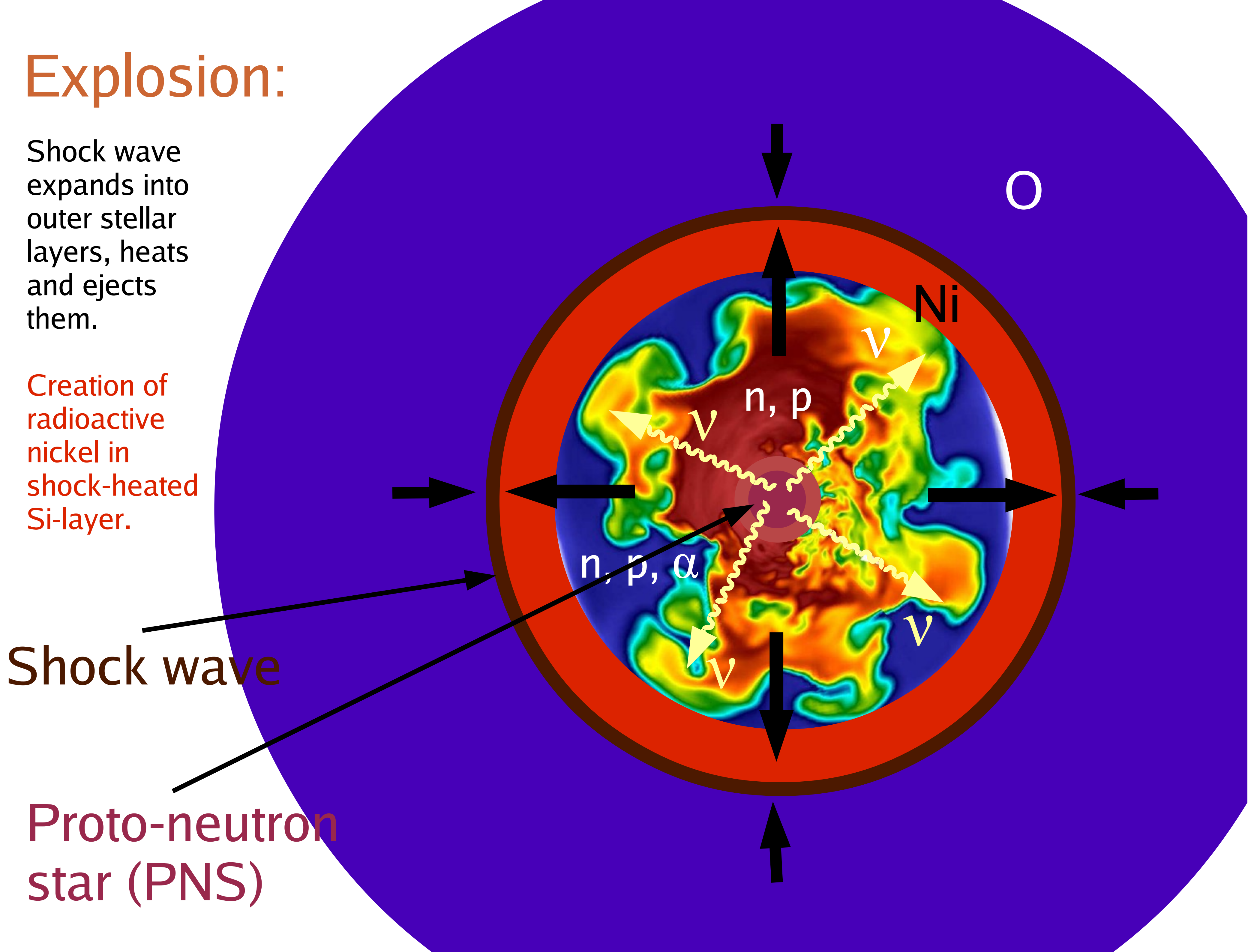

Nucleosynthesis during the explosion:

Shock-heated and neutrino-heated outflows are sites for element formation

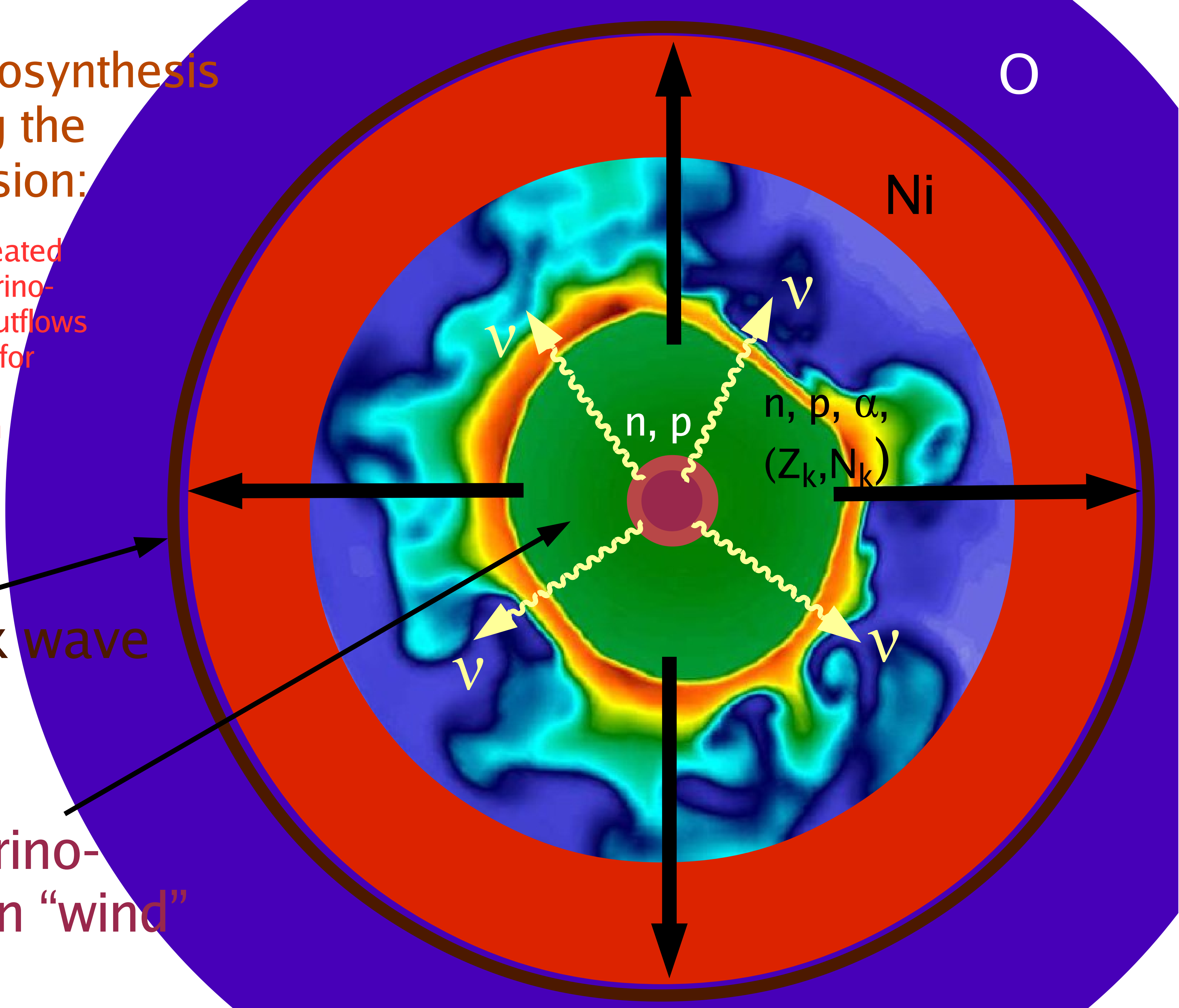

Neutrinos & SN Explosion Mechanism

Paradigm: Explosions by the neutrino-heating mechanism, supported by hydrodynamic instabilities in the postshock layer

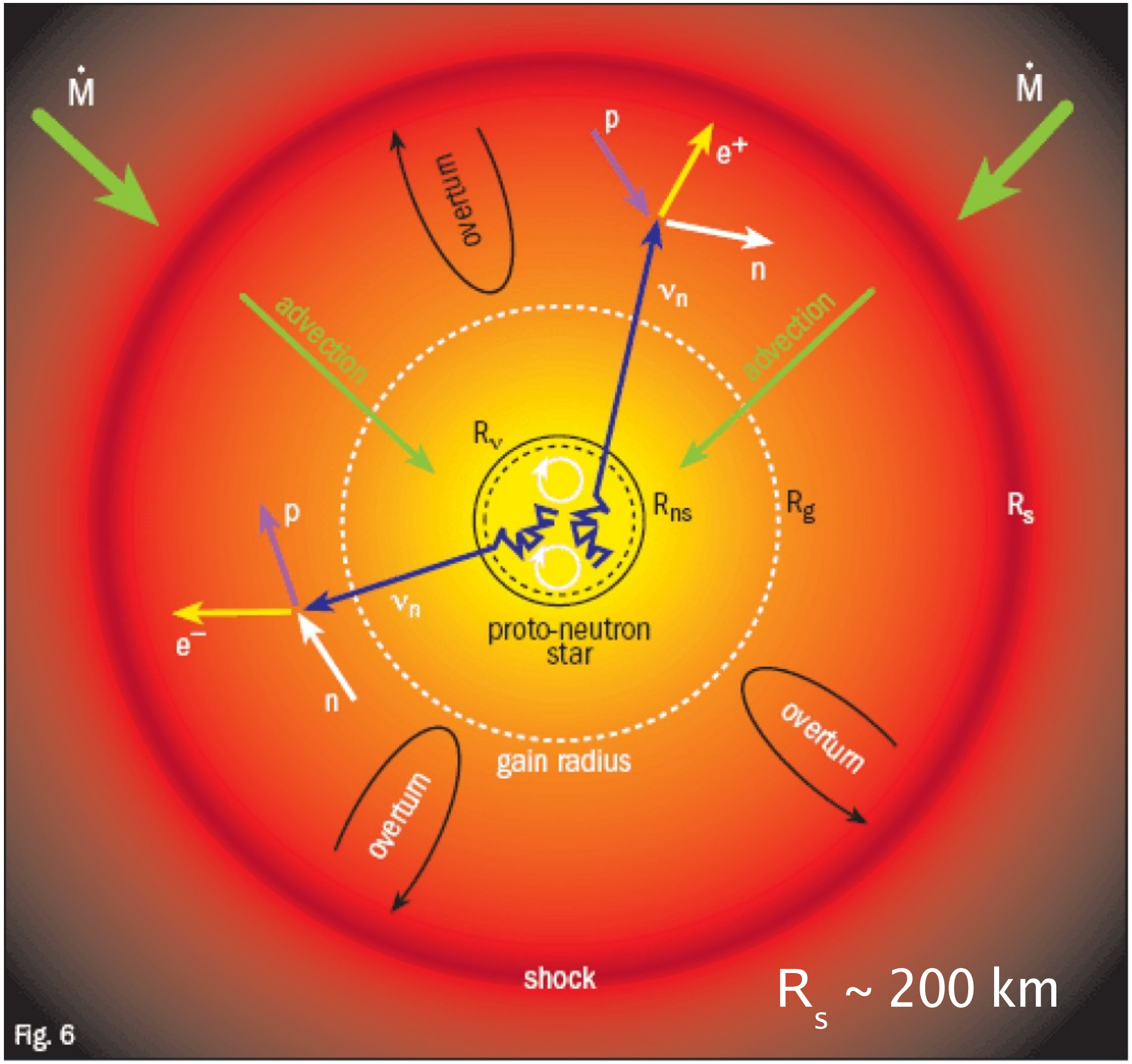

- "Neutrino-heating mechanism": Neutrinos `revive' stalled shock by energy deposition (Colgate & White 1966, Wilson 1982, Bethe & Wilson 1985);
- Convective processes & hydrodynamic instabilities support the heating mechanism (Herant et al. 1992, 1994; Burrows et al. 1995, Janka & Müller 1994, 1996; Fryer & Warren 2002, 2004; Blondin et al. 2003; Scheck et al. 2004,06,08, Iwakami et al. 2008, 2009, Ohnishi et al. 2006).

Neutrino Heating and Cooling

$$\boxed{\begin{aligned} \nu_e + n &\rightarrow e^- + p \\ \bar{\nu}_e + p &\rightarrow e^+ + n \end{aligned}}$$

- Neutrino heating:

$$q_\nu^+ = 1.544 \times 10^{20} \left(\frac{L_{\nu_e}}{10^{52}\ \mathrm{erg\ s^{-1}}}\right)\left(\frac{T_{\nu_e}}{4\ \mathrm{MeV}}\right)^2 \times \left(\frac{100\ \mathrm{km}}{r}\right)^2 (Y_n + Y_p) \qquad \left[\frac{\mathrm{erg}}{\mathrm{g\ s}}\right]$$

- Neutrino cooling:

$$\mathcal{C} = 1.399 \times 10^{20} \left(\frac{T}{2\ \mathrm{MeV}}\right)^6 (Y_n + Y_p) \qquad \left[\frac{\mathrm{erg}}{\mathrm{g\ s}}\right]$$

$$\begin{aligned} Q_\nu^+ &= q_\nu^+ M_g \\ &\sim 9.4 \times 10^{51}\ \frac{\mathrm{erg}}{\mathrm{s}} \left(\frac{k_B T_\nu}{4\ \mathrm{MeV}}\right)^2 \left(\frac{L_\nu}{3 \cdot 10^{52}\ \mathrm{erg/s}}\right)\left(\frac{M_g}{0.01\ M_\odot}\right)\left(\frac{R_g}{100\ \mathrm{km}}\right)^{-2} \end{aligned}$$

$$\boxed{\begin{aligned} E_N &\sim Q_\nu^+ t_{\mathrm{dwell}} \\ &\sim 9.4 \times 10^{50}\ \mathrm{erg} \left(\frac{k_B T_\nu}{4\ \mathrm{MeV}}\right)^2 \left(\frac{L_\nu}{3 \cdot 10^{52}\ \mathrm{erg/s}}\right) \times \\ &\qquad \left(\frac{M_g}{0.01\ M_\odot}\right)^2 \left(\frac{\dot{M}}{0.1\ M_\odot\ \mathrm{s^{-1}}}\right)^{-1} \left(\frac{R_g}{100\ \mathrm{km}}\right)^{-2} \end{aligned}}$$

$$\boxed{t_{\mathrm{dwell}} \approx \frac{M_g}{\dot{M}}}$$

Hydrodynamic instabilities

See, e.g., Janka, ARNPS 62 (2012) 407

1D-2D Differences in Parametric Explosion Models

- Nordhaus et al. (ApJ 720 (2010) 694) and Murphy & Burrows (2008) performed 1D & 2D simulations with simple neutrino- heating and cooling terms (no neutrino transport but lightbulb) and found up to ~30% improvement in 2D for 15 M_{sun} progenitor star.

$$\mathcal{H} = 1.544 \times 10^{20} \left(\frac{L_{\nu_e}}{10^{52}\ \mathrm{erg\ s^{-1}}} \right) \left(\frac{T_{\nu_e}}{4\ \mathrm{MeV}} \right)^2 \times \left(\frac{100\,\mathrm{km}}{r} \right)^2 (Y_\mathrm{n} + Y_\mathrm{p}) e^{-\tau_{\nu_e}} \left[\frac{\mathrm{erg}}{\mathrm{g\ s}} \right]$$

$$\mathcal{C} = 1.399 \times 10^{20} \left(\frac{T}{2\ \mathrm{MeV}} \right)^6 (Y_\mathrm{n} + Y_\mathrm{p}) e^{-\tau_{\nu_e}} \left[\frac{\mathrm{erg}}{\mathrm{g\ s}} \right]$$

(ApJ 720 (2010) 694)

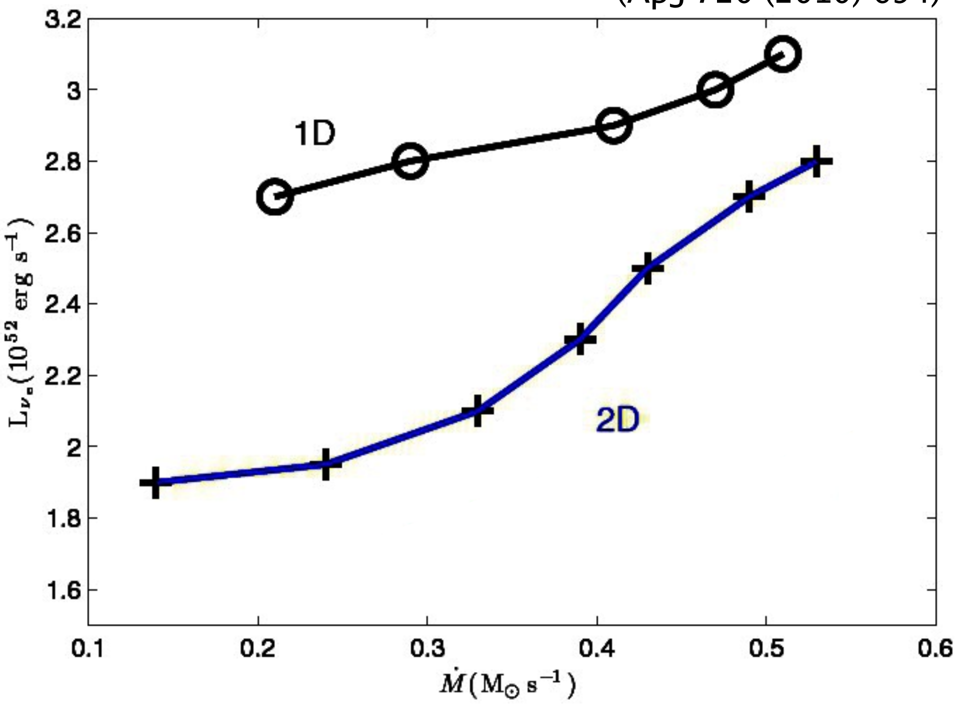

But: Is neutrino heating strong enough to initiate the explosion?

Most sophisticated, self-consistent numerical simulations of the explosion mechanism in 2D and 3D are necessary!

Predictions of Signals from SN Core

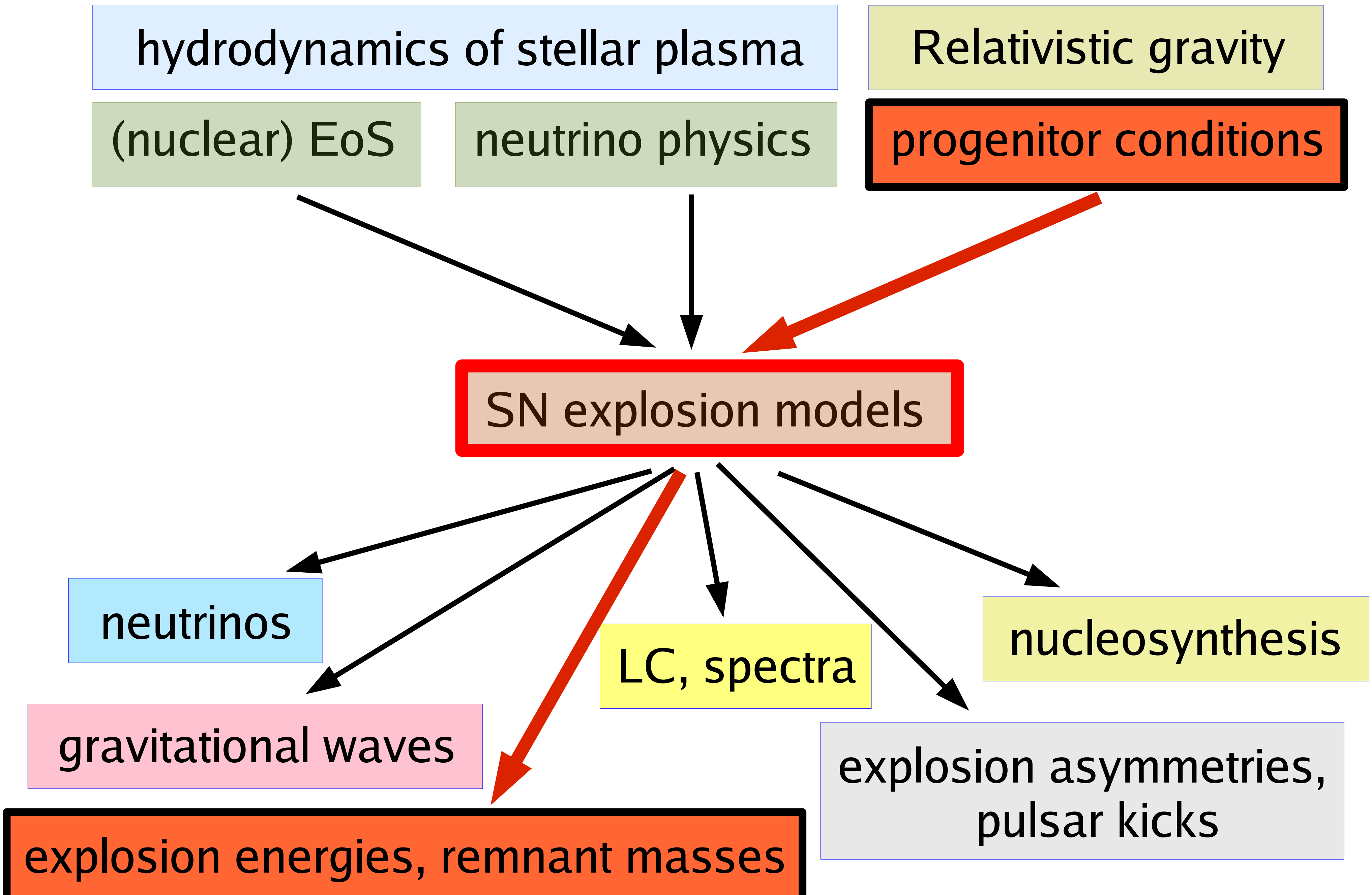

Explosion Mechanism: Most Sophisticated Current Models

General-Relativistic 2D Supernova Models of the Garching Group

(Müller B., PhD Thesis (2009); Müller et al., ApJS, (2010))

GR hydrodynamics (CoCoNuT)

$$
\begin{aligned}
\frac{\partial\sqrt{\gamma}\rho W}{\partial t}+\frac{\partial\sqrt{-g}\rho W\hat{v}^i}{\partial x^i} &= 0, && (2.5)\\
\frac{\partial\sqrt{\gamma}\rho h W^2 v_j}{\partial t}+\frac{\partial\sqrt{-g}\left(\rho h W^2 v_j\hat{v}^i+\delta^i_j P\right)}{\partial x^i} &= \frac{1}{2}\sqrt{-g}T^{\mu\nu}\frac{\partial g_{\mu\nu}}{\partial x^j}+\left(\frac{\partial\sqrt{\gamma}S_j}{\partial t}\right)_C, && (2.6)\\
\frac{\partial\sqrt{\gamma}\tau}{\partial t}+\frac{\partial\sqrt{-g}\left(\tau\hat{v}^i+Pv^i\right)}{\partial x^i} &= \alpha\sqrt{-g}\left(T^{\mu 0}\frac{\partial\ln\alpha}{\partial x^\mu}-T^{\mu\nu}\Gamma^0_{\mu\nu}\right)+\left(\frac{\partial\sqrt{\gamma}\tau}{\partial t}\right)_C. && (2.7)
\end{aligned}
$$

$$
\frac{\partial\sqrt{\gamma}\rho W Y_e}{\partial t}+\frac{\partial\sqrt{-g}\rho W Y_e\hat{v}^i}{\partial x^i}=\left(\frac{\partial\sqrt{\gamma}\rho W Y_e}{\partial t}\right)_C, \qquad (2.8)
$$

$$
\frac{\partial\sqrt{\gamma}\rho W X_k}{\partial t}+\frac{\partial\sqrt{-g}\rho W X_k\hat{v}^i}{\partial x^i}=0. \qquad (2.9)
$$

CFC metric equations

$$
\begin{aligned}
\hat{\Delta}\Phi &= -2\pi\phi^5\left(E+\frac{K_{ij}K^{ij}}{16\pi}\right), && (2.10)\\
\hat{\Delta}(\alpha\Phi) &= 2\pi\alpha\phi^5\left(E+2S+\frac{7K_{ij}K^{ij}}{16\pi}\right), && (2.11)\\
\hat{\Delta}\beta^i &= 16\pi\alpha\phi^4S^i+2\phi^{10}K^{ij}\hat{\nabla}_j\left(\frac{\alpha}{\Phi^6}\right)-\frac{1}{3}\hat{\nabla}^i\hat{\nabla}_j\beta^j, && (2.12)
\end{aligned}
$$

$$
\begin{aligned}
&\frac{\partial W\left(\hat{J}+v_r\hat{H}\right)}{\partial t}+\frac{\partial}{\partial r}\left[\left(W\frac{\alpha}{\phi^2}-\beta_r v_r\right)\hat{H}+\left(Wv_r\frac{\alpha}{\phi^2}-\beta_r\right)\hat{J}\right]- \qquad (2.28)\\
&\frac{\partial}{\partial\varepsilon}\left\{W\varepsilon\hat{J}\left[\frac{1}{r}\left(\beta_r-\frac{\alpha v_r}{\phi^2}\right)+2\left(\beta_r-\frac{\alpha v_r}{\phi^2}\right)\frac{\partial\ln\phi}{\partial r}-2\frac{\partial\ln\phi}{\partial t}\right]+\right.\\
&W\varepsilon\hat{H}\left[v_r\left(\frac{\partial\beta_r\phi^2}{\partial r}-2\frac{\partial\ln\phi}{\partial t}\right)-\frac{\alpha}{\phi^2}\frac{\partial\ln\alpha W}{\partial r}+\alpha W^2\left(\beta_r\frac{\partial v_r}{\partial r}-\frac{\partial v_r}{\partial t}\right)\right]-\\
&\left.\varepsilon\hat{K}\left[\frac{\beta_r W}{r}-\frac{\partial\beta_r W}{\partial r}+Wv_r r\frac{\partial}{\partial r}\left(\frac{\alpha}{r\phi^2}\right)+W^3\left(\frac{\alpha}{\phi^2}\frac{\partial v_r}{\partial r}+v_r\frac{\partial v_r}{\partial t}\right)\right]\right\}-\\
&W\hat{J}\left[\frac{1}{r}\left(\beta_r-\frac{\alpha v_r}{\phi^2}\right)+2\left(\beta_r-\frac{\alpha v_r}{\phi^2}\right)\frac{\partial\ln\phi}{\partial r}-2\frac{\partial\ln\phi}{\partial t}\right]-\\
&W\hat{H}\left[v_r\left(\frac{\partial\beta_r\phi^2}{\partial r}-2\frac{\partial\ln\phi}{\partial t}\right)-\frac{\alpha}{\phi^2}\frac{\partial\ln\alpha W}{\partial r}+\alpha W^2\left(\beta_r\frac{\partial v_r}{\partial r}-\frac{\partial v_r}{\partial t}\right)\right]+\\
&\hat{K}\left[\frac{\beta_r W}{r}-\frac{\partial\beta_r W}{\partial r}+Wv_r r\frac{\partial}{\partial r}\left(\frac{\alpha}{r\phi^2}\right)+W^3\left(\frac{\alpha}{\phi^2}\frac{\partial v_r}{\partial r}+v_r\frac{\partial v_r}{\partial t}\right)\right]=\alpha\hat{C}^{(0)},
\end{aligned}
$$

$$
\begin{aligned}
&\frac{\partial W\left(\hat{H}+v_r\hat{K}\right)}{\partial t}+\frac{\partial}{\partial r}\left[\left(W\frac{\alpha}{\phi^2}-\beta_r v_r\right)\hat{K}+\left(Wv_r\frac{\alpha}{\phi^2}-\beta_r\right)\hat{H}\right]- \qquad (2.29)\\
&\frac{\partial}{\partial\varepsilon}\left\{W\varepsilon\hat{H}\left[\frac{1}{r}\left(\beta_r-\frac{\alpha v_r}{\phi^2}\right)+2\left(\beta_r-\frac{\alpha v_r}{\phi^2}\right)\frac{\partial\ln\phi}{\partial r}-2\frac{\partial\ln\phi}{\partial t}\right]+\right.\\
&W\varepsilon\hat{K}\left[v_r\left(\frac{\partial\beta_r\phi^2}{\partial r}-2\frac{\partial\ln\phi}{\partial t}\right)-\frac{\alpha}{\phi^2}\frac{\partial\ln\alpha W}{\partial r}+\alpha W^2\left(\beta_r\frac{\partial v_r}{\partial r}-\frac{\partial v_r}{\partial t}\right)\right]-\\
&\left.\varepsilon\hat{L}\left[\frac{\beta_r W}{r}-\frac{\partial\beta_r W}{\partial r}+Wv_r r\frac{\partial}{\partial r}\left(\frac{\alpha}{r\phi^2}\right)+W^3\left(\frac{\alpha}{\phi^2}\frac{\partial v_r}{\partial r}+v_r\frac{\partial v_r}{\partial t}\right)\right]\right\}+\\
&\left(\hat{J}-\hat{K}\right)\left[v_r\left(\frac{\beta_r}{r}-\frac{\partial\beta_r}{\partial r}\right)+\frac{\partial}{\partial r}\left(\frac{W\alpha}{\phi^2}\right)-\frac{W\alpha}{r\phi^2}+W^3\left(\frac{\partial v_r}{\partial t}-\beta_r\frac{\partial v_r}{\partial r}\right)\right]+\\
&\left(\hat{H}-\hat{L}\right)\left[\frac{W^3\alpha}{\phi^2}\frac{\partial v_r}{\partial r}+\frac{\beta W}{r}-\frac{\partial\beta W}{\partial r}-Wv_r r\frac{\partial}{\partial r}\left(\frac{\alpha}{r\phi^2}\right)+\frac{\partial W}{\partial t}\right]-\\
&W\hat{H}\left[\frac{1}{r}\left(\beta_r-\frac{\alpha v_r}{\phi^2}\right)+2\left(\beta_r-\frac{\alpha v_r}{\phi^2}\right)\frac{\partial\ln\phi}{\partial r}-2\frac{\partial\ln\phi}{\partial t}\right]-\\
&W\hat{K}\left[v_r\left(\frac{\partial\beta_r\phi^2}{\partial r}-2\frac{\partial\ln\phi}{\partial t}\right)-\frac{\alpha}{\phi^2}\frac{\partial\ln\alpha W}{\partial r}+\alpha W^2\left(\beta_r\frac{\partial v_r}{\partial r}-\frac{\partial v_r}{\partial t}\right)\right]+\\
&\hat{L}\left[\frac{\beta_r W}{r}-\frac{\partial\beta_r W}{\partial r}+Wv_r r\frac{\partial}{\partial r}\left(\frac{\alpha}{r\phi^2}\right)+W^3\left(\frac{\alpha}{\phi^2}\frac{\partial v_r}{\partial r}+v_r\frac{\partial v_r}{\partial t}\right)\right]=\alpha\hat{C}^{(1)}.
\end{aligned}
$$

Neutrino transport (VERTEX)

Neutrino Reactions in Supernovae

Beta processes:

- $e^- + p \rightleftharpoons n + \nu_e$
- $e^+ + n \rightleftharpoons p + \bar{\nu}_e$
- $e^- + A \rightleftharpoons \nu_e + A^*$

Neutrino scattering:

- $\nu + n, p \rightleftharpoons \nu + n, p$
- $\nu + A \rightleftharpoons \nu + A$
- $\nu + e^\pm \rightleftharpoons \nu + e^\pm$

Thermal pair processes:

- $N + N \rightleftharpoons N + N + \nu + \bar{\nu}$
- $e^+ + e^- \rightleftharpoons \nu + \bar{\nu}$

Neutrino-neutrino reactions:

- $\nu_x + \nu_e, \bar{\nu}_e \rightleftharpoons \nu_x + \nu_e, \bar{\nu}_e$
  $(\nu_x = \nu_\mu, \bar{\nu}_\mu, \nu_\tau, \text{or } \bar{\nu}_\tau)$
- $\nu_e + \bar{\nu}_e \rightleftharpoons \nu_{\mu,\tau} + \bar{\nu}_{\mu,\tau}$

The Curse and Challenge of the Dimensions

Boltzmann equation determines neutrino distribution function in 6D phase space and time

$$f\left(r,\theta,\phi,\Theta,\Phi,\epsilon,t\right)$$

Integration over 3D momentum space yields source terms for hydrodynamics

$$Q\left(r,\theta,\phi,t\right),\dot{Y}_e\left(r,\theta,\phi,t\right)$$

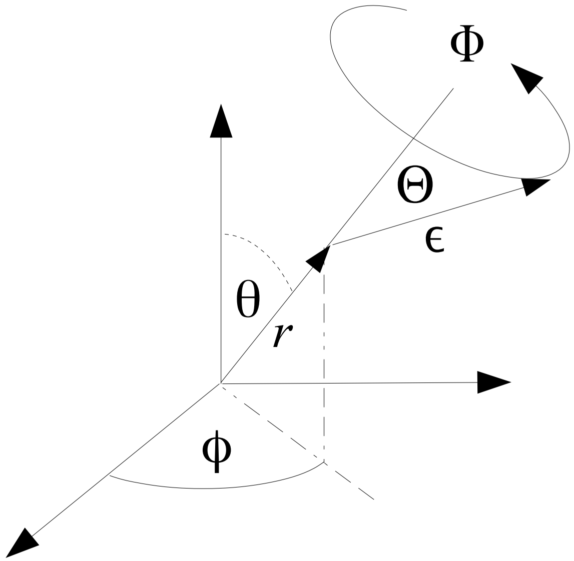

Solution approach	Required resources
• **3D** hydro + **6D** direct discretization of Boltzmann Eq. (code development by Sumiyoshi & Yamada '12)	• ≥ 10–100 PFlops/s (sustained!)
• **3D** hydro + two-moment closure of Boltzmann Eq. (next feasible step to full 3D; cf. Kuroda et al. 2012)	• ≥ 1–10 Pflops/s, TBytes
• **3D** hydro + "**ray-by-ray-plus**" variable Eddington factor method (method used at MPA/Garching)	• ≥ 0.1–1 PFlops/s, Tbytes
• **2D** hydro + "**ray-by-ray-plus**" variable Eddington factor method (method used at MPA/Garching)	• ≥ 0.1–1 Tflops/s, < 1 TByte

"Ray-by-Ray" Approximation for Neutrino Transport in 2D and 3D Geometry

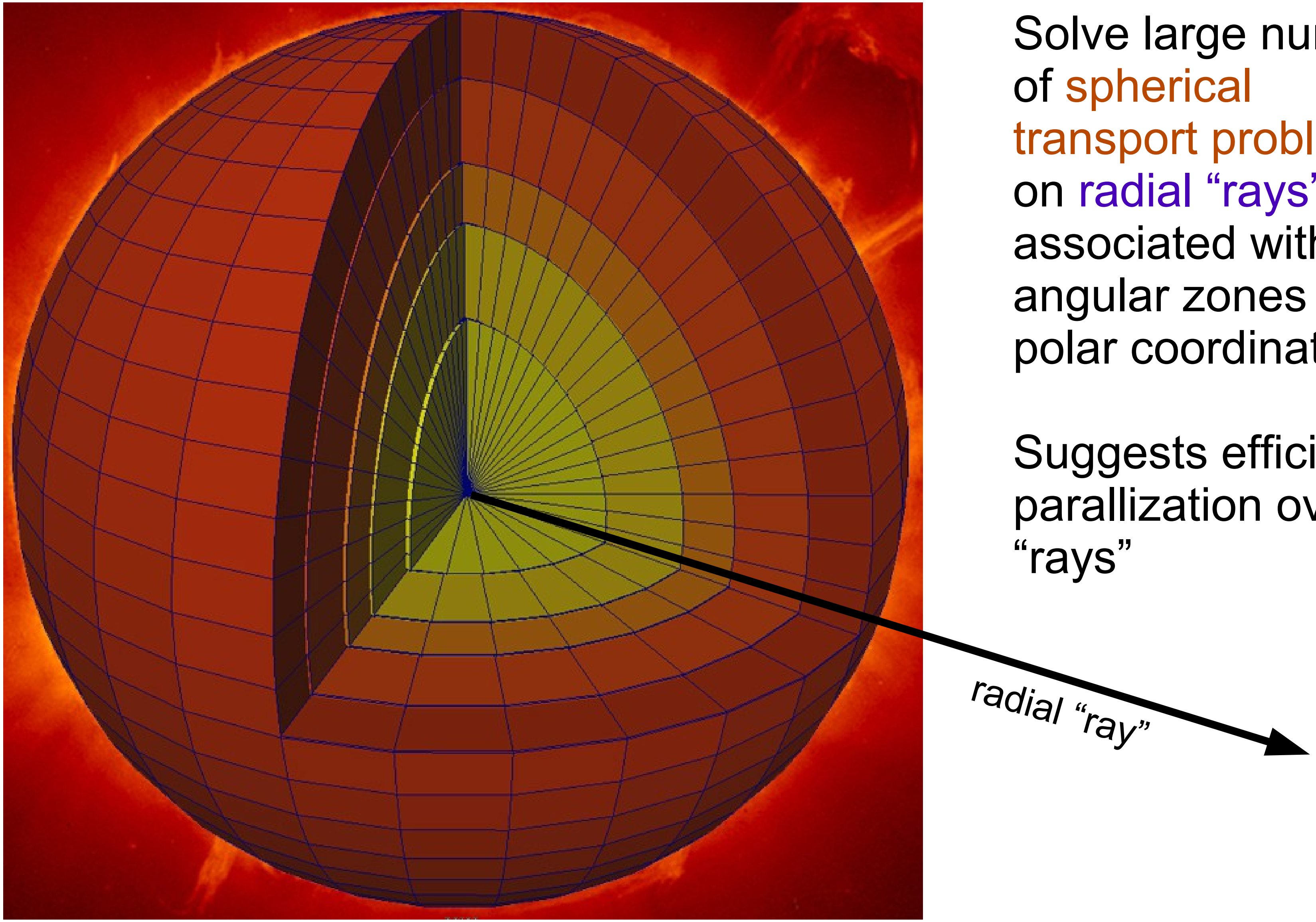

Solve large number of spherical transport problems on radial “rays” associated with angular zones of polar coordinate grid

Suggests efficient parallization over the “rays”

Performance and Portability of our Supernova Code *Prometheus-Vertex*

- Code employs hybrid MPI/OpenMP programming model (collaborative development with **Katharina Benkert, HLRS**).
- Code has been ported to different computer platforms by **Andreas Marek, High Level Application Support, Rechenzentrum Garching (RZG).**
- Code shows excellent parallel efficiency, which will be fully exploited in 3D.

Strong Scaling

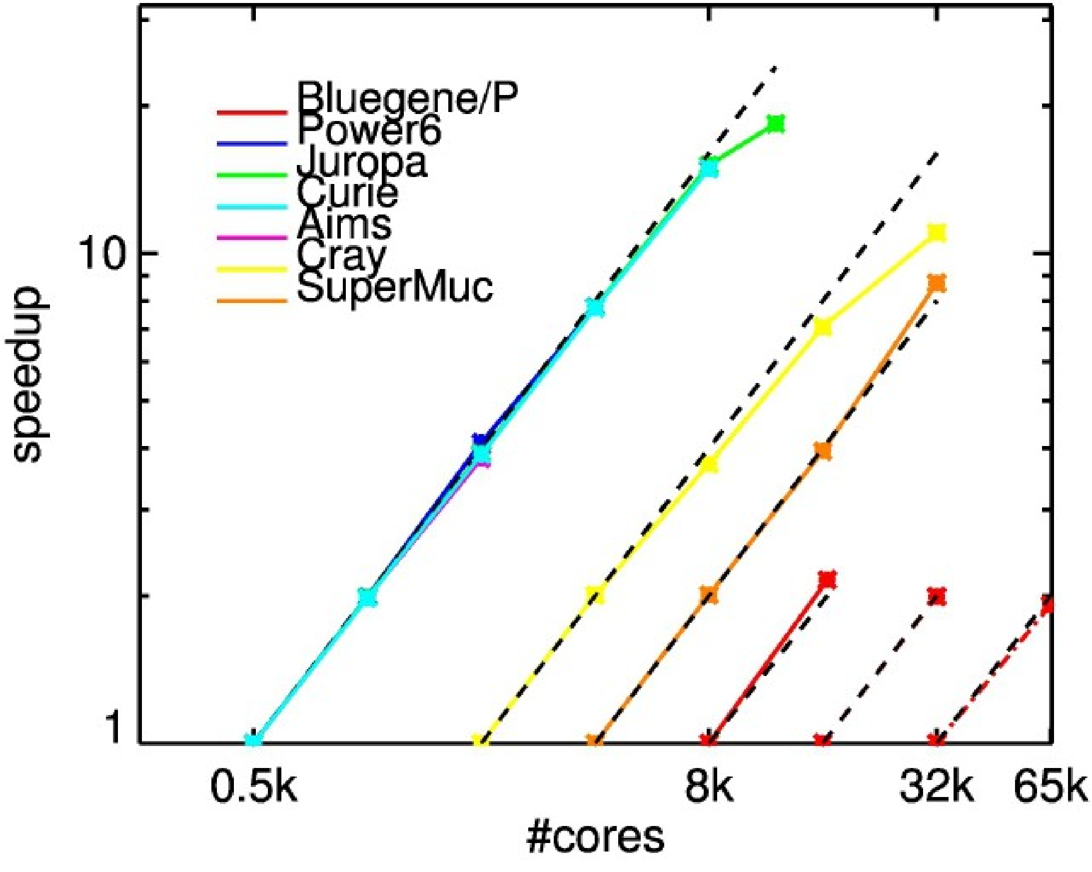

Andreas Marek, RZG (2012)

Relativistic 2D CCSN Explosion Models

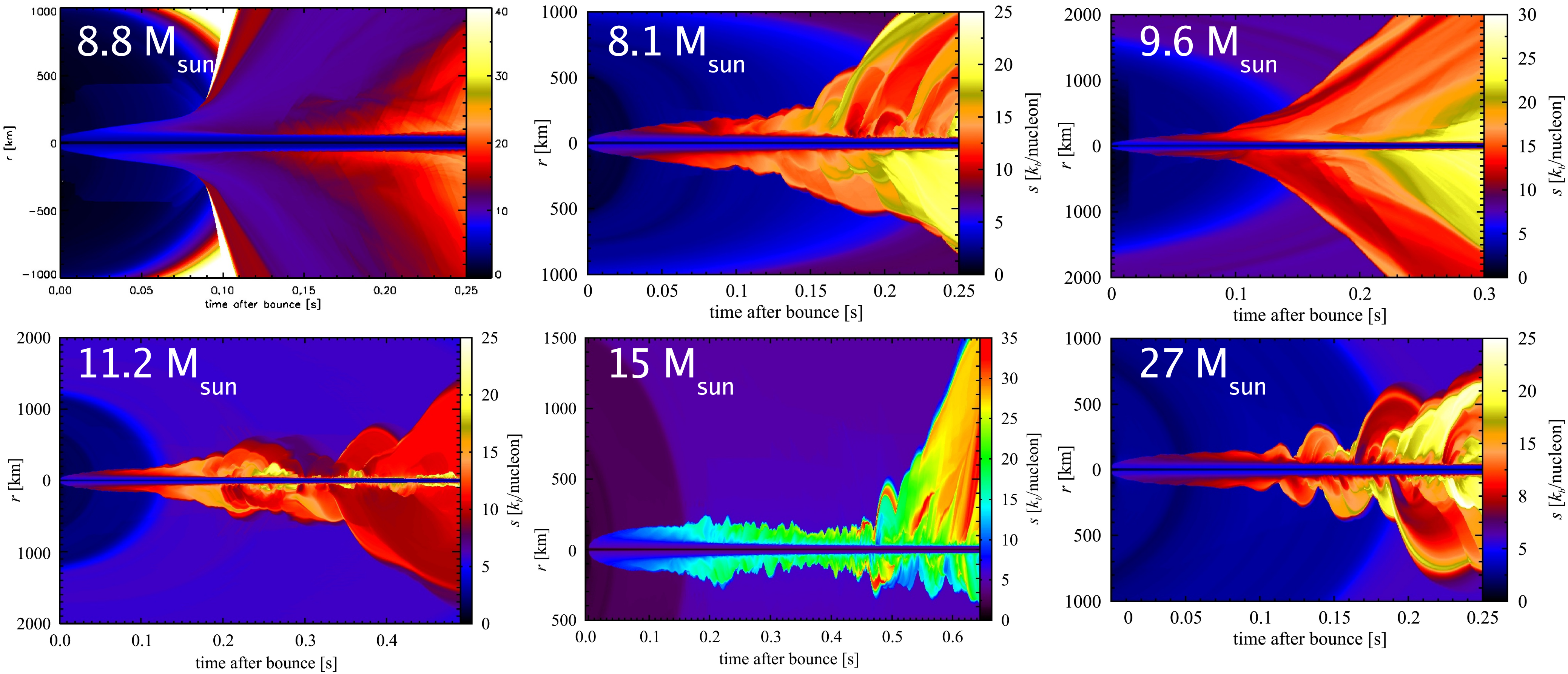

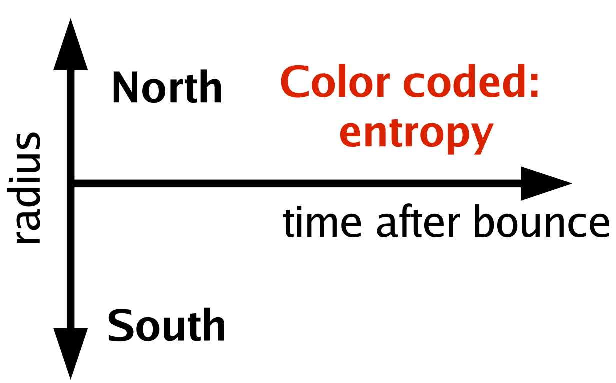

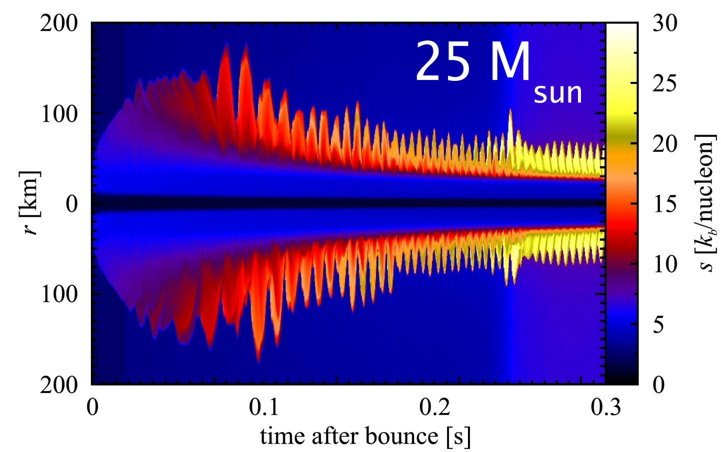

Bernhard Müller, THJ, et al. (ApJ 756, ApJ 761, arXiv:1210.6984

Basic confirmation of previous explosion models for 11.2 and 15 M_{sun} stars by Marek & THJ (2009)

Relativistic 2D CCSN Explosion Models

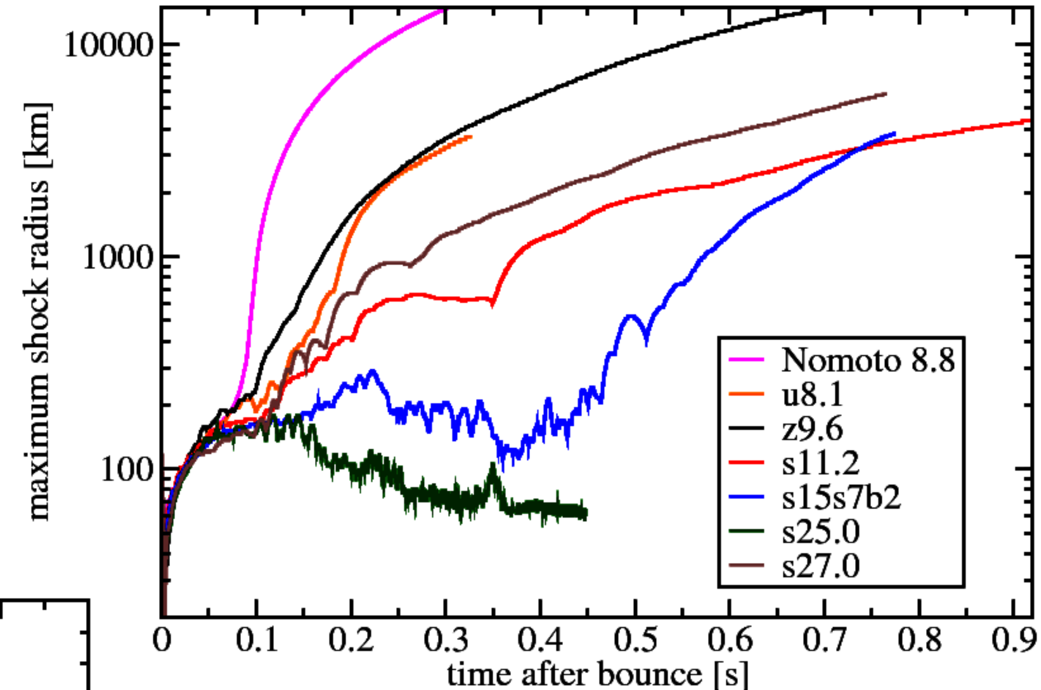

Maximum shock radius

"Diagnostic energy" of explosion

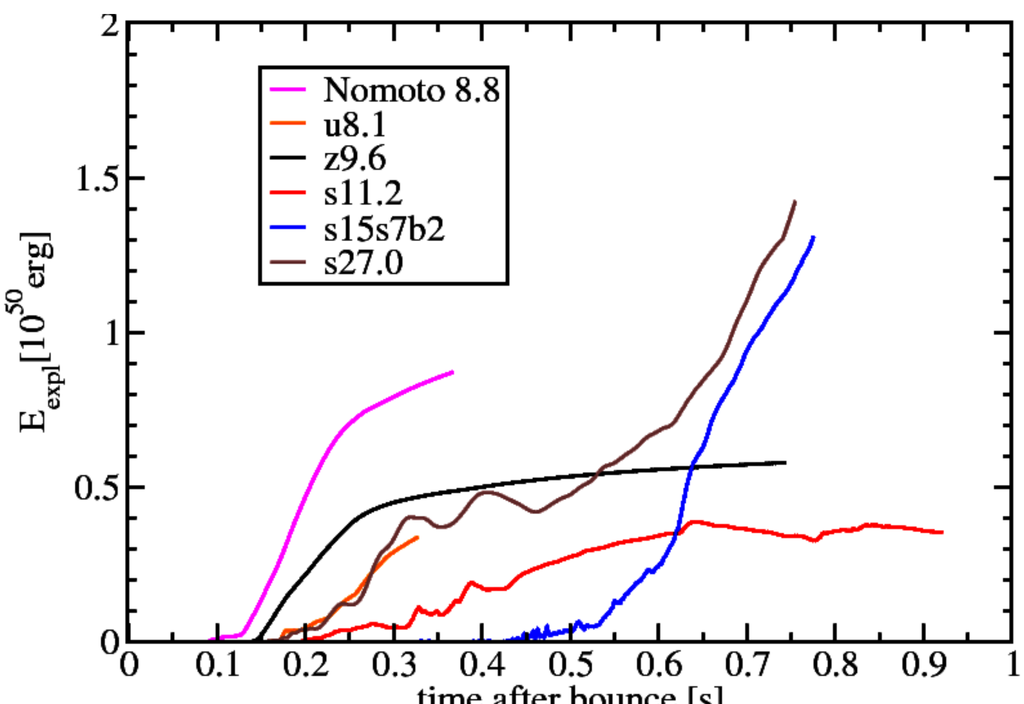

2D SN Explosion Models

- Basic confirmation of the neutrino-driven mechanism
- Confirm reduction of the critical neutrino luminosity that enables an explosion in self-consistent 2D treatments compared to 1D

Nucleosynthesis in Neutrino-Heated SN Ejecta

Crucial parameters for nucleosynthesis in neutrino-driven outflows:

* Electron-to-baryon ratio Y_e (<---> neutron excess)
* Entropy (<----> ratio of (temperature)^3 to density)
* Expansion timescale

Determined by the interaction of stellar gas with neutrinos from nascent neutron star:

$$\nu_\mathrm{e} + n \rightarrow e^- + p$$
$$\bar{\nu}_\mathrm{e} + p \rightarrow e^+ + n$$

$$\boxed{Y_e \sim \left[1 + \frac{L_{\bar{\nu}_e}(\epsilon_{\bar{\nu}_e} - 2\Delta)}{L_{\nu_e}(\epsilon_{\nu_e} + 2\Delta)}\right]^{-1}}$$

$$\text{with} \quad \epsilon_\nu = \frac{\langle \epsilon_\nu^2 \rangle}{\langle \epsilon_\nu \rangle} \quad \text{and} \quad \Delta = (m_n - m_p)c^2 \approx 1.29\,\mathrm{MeV}.$$

If $L_{\bar{\nu}_e} \approx L_{\nu_e}$, one needs for $Y_e < 0.5$ (i.e. neutron excess):

$$\boxed{\epsilon_{\bar{\nu}_e} - \epsilon_{\nu_e} > 4\Delta.}$$

Nucleosynthesis in Neutrino-Heated SN Ejecta

Convectively ejected n-rich matter makes ONeMg-core and low-mass Fe-core supernovae an interesting source of nuclei between the iron group and N = 50 (from Zn to Zr), possibly also of weak r-process nuclei.

(Wanajo, THJ, Müller, ApJL 726, L15 (2011))

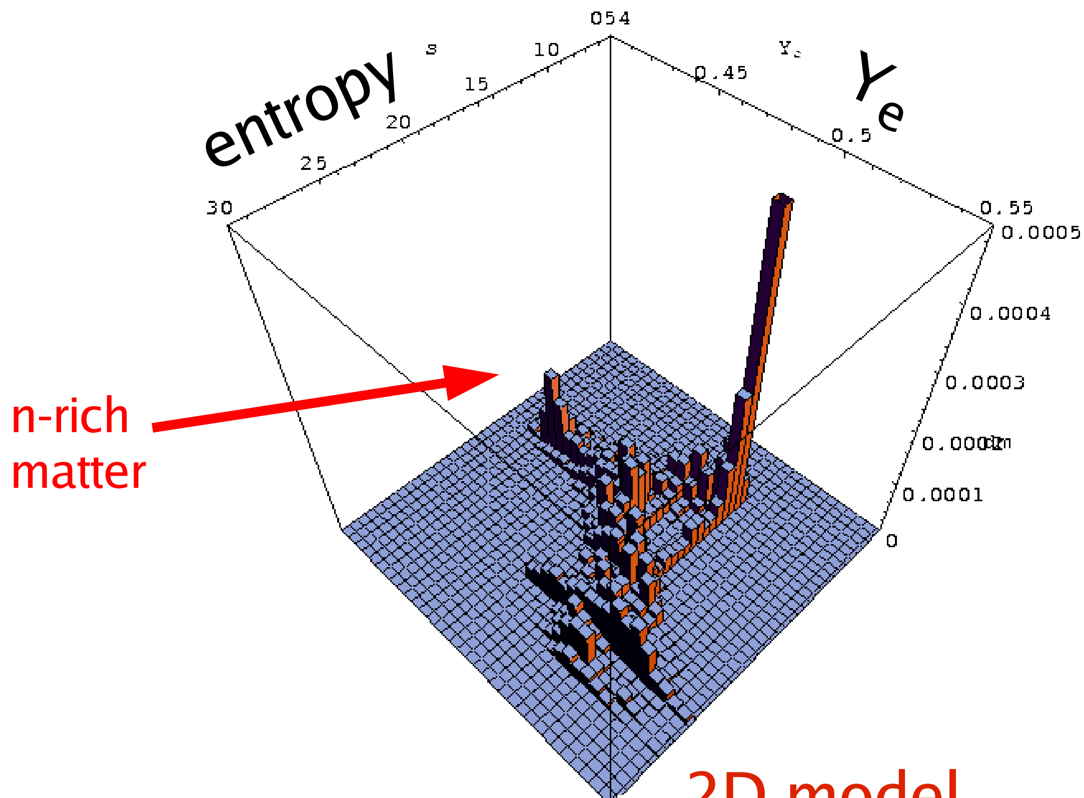

2D model

9.6 M_{sun} (z=0) Fe core SN

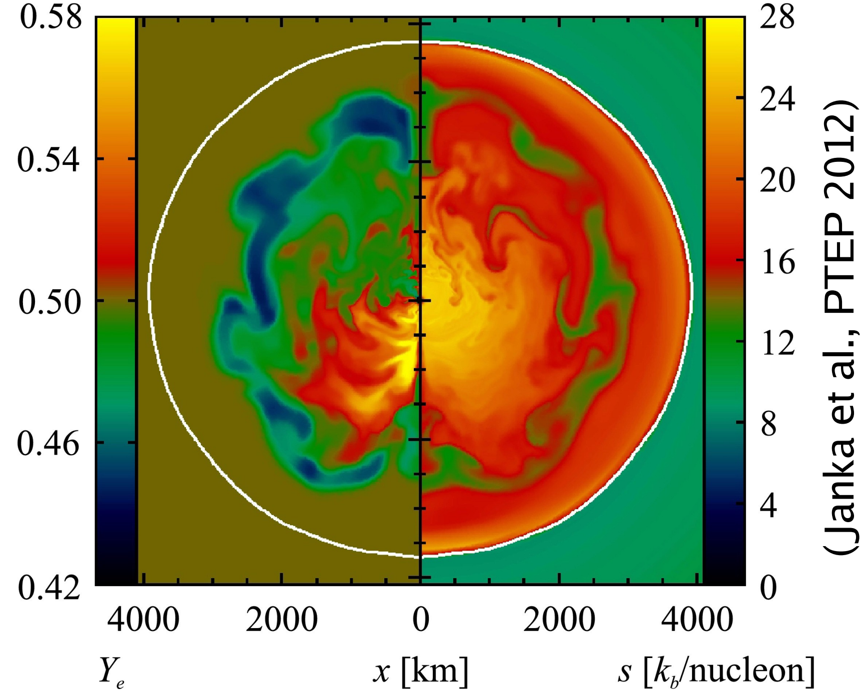

8.8 M_{sun} O-Ne-Mg core SN

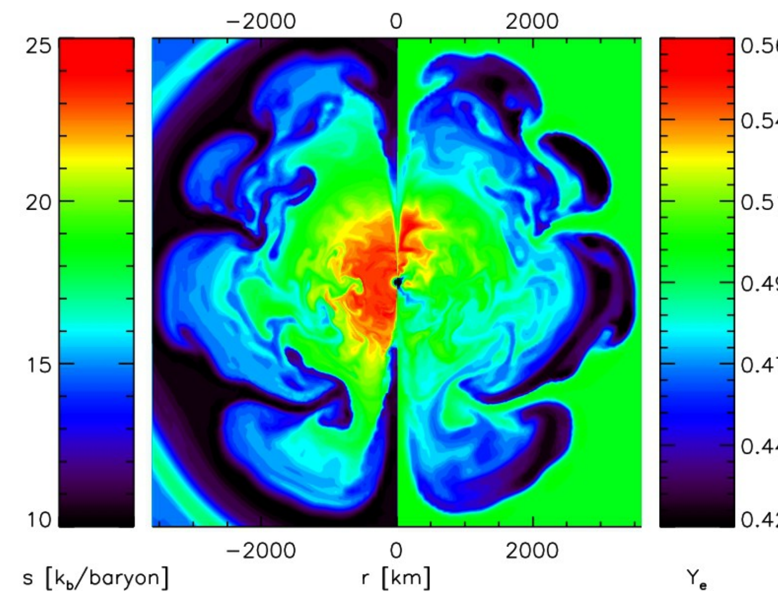

Support for 2D CCSN Explosion Models

AXISYMMETRIC *AB INITIO* CORE-COLLAPSE SUPERNOVA SIMULATIONS OF 12–25 $M_\odot$ STARS

STEPHEN W. BRUENN[1], ANTHONY MEZZACAPPA[2,3,4], W. RAPHAEL HIX[2,3], ERIC J. LENTZ[3,2,5], O. E. BRONSON MESSER[6,3,4], ERIC J. LINGERFELT[2,4], JOHN M. BLONDIN[7], EIRIK ENDEVE[4], PEDRO MARRONETTI[1,8], AND KONSTANTIN N. YAKUNIN[1]

2D explosions for 12, 15, 20, 25 M_{sun} progenitors of Woosley & Heger (2007)

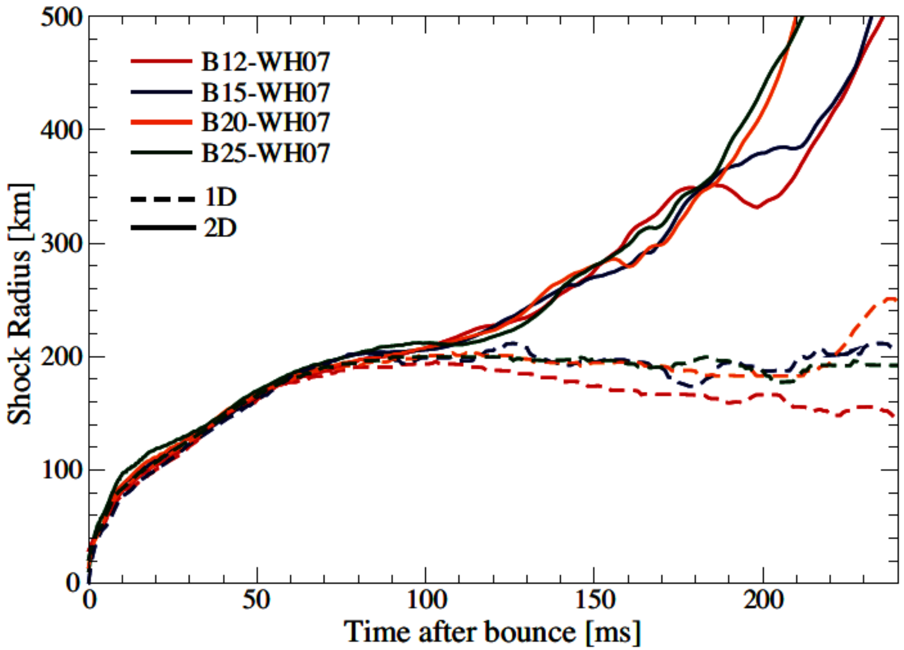

Bruenn et al., arXiv:1212.1747

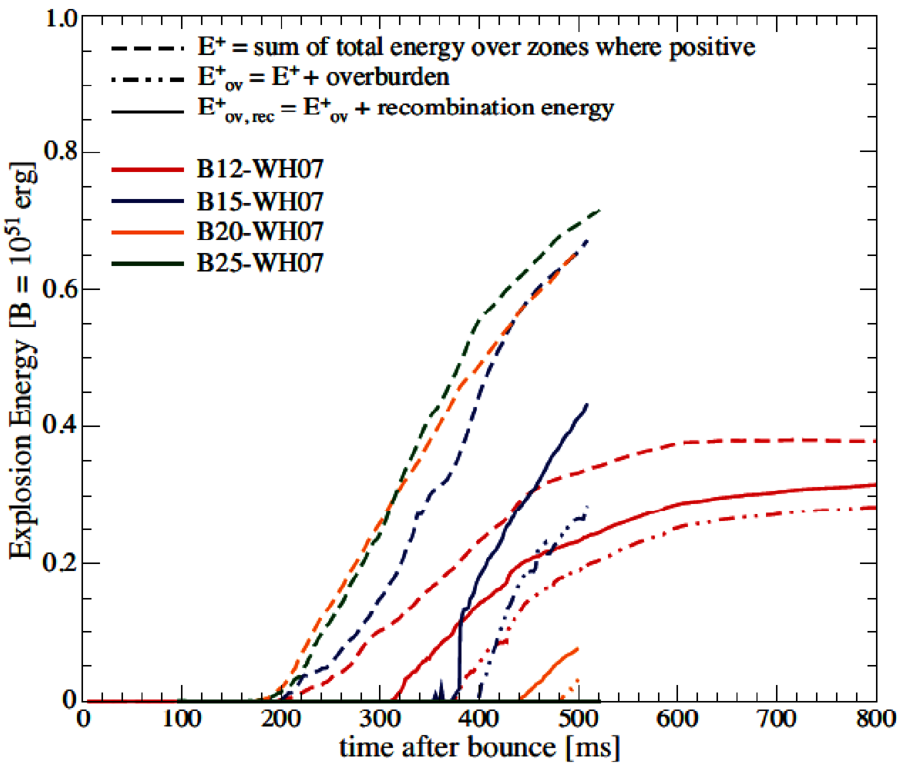

2D SN Explosion Models

Results and numerical approaches of different groups still differ in many aspects:

- **Different explosion behavior and different explosion energies**
- **Different codes, neutrino transport schems and reactions, EoS treatment**

<u>Direct</u> comparisons are urgently needed!

Challenge and Goal: 3D

- 2D explosions seem to be "marginal", at least for some progenitor models and in some (the most?) sophisticated simulations.
- Nature is three dimensional, but 2D models impose the constraint of axisymmetry.
- Turbulent cascade in 3D transports energy from large to small scales, which is opposite to 2D.
- Is 3D turbulence more supportive to an explosion?
  Is the third dimension the key to the neutrino mechanism?
- 3D models are needed to confirm explosion mechanism suggested by 2D simulations!

3D vs. 2D Differences:

The Dimension Conundrum

2D-3D Differences in Parametric Explosion Models

- Nordhaus et al. (ApJ 720 (2010) 694) performed 2D & 3D simulations with simple neutrino- heating and cooling terms (no neutrino transport but lightbulb) and found 15–25% improvement in 3D for 15 M_{sun} progenitor star (ApJ 720 (2010) 694)

$$\mathcal{H} = 1.544 \times 10^{20} \left(\frac{L_{\nu_e}}{10^{52}\ \mathrm{erg\ s^{-1}}}\right)\left(\frac{T_{\nu_e}}{4\ \mathrm{MeV}}\right)^2 \times \left(\frac{100\ \mathrm{km}}{r}\right)^2 (Y_\mathrm{n} + Y_\mathrm{p}) e^{-\tau_{\nu_e}} \left[\frac{\mathrm{erg}}{\mathrm{g\ s}}\right]$$

$$\mathcal{C} = 1.399 \times 10^{20} \left(\frac{T}{2\ \mathrm{MeV}}\right)^6 (Y_\mathrm{n} + Y_\mathrm{p}) e^{-\tau_{\nu_e}} \left[\frac{\mathrm{erg}}{\mathrm{g\ s}}\right]$$

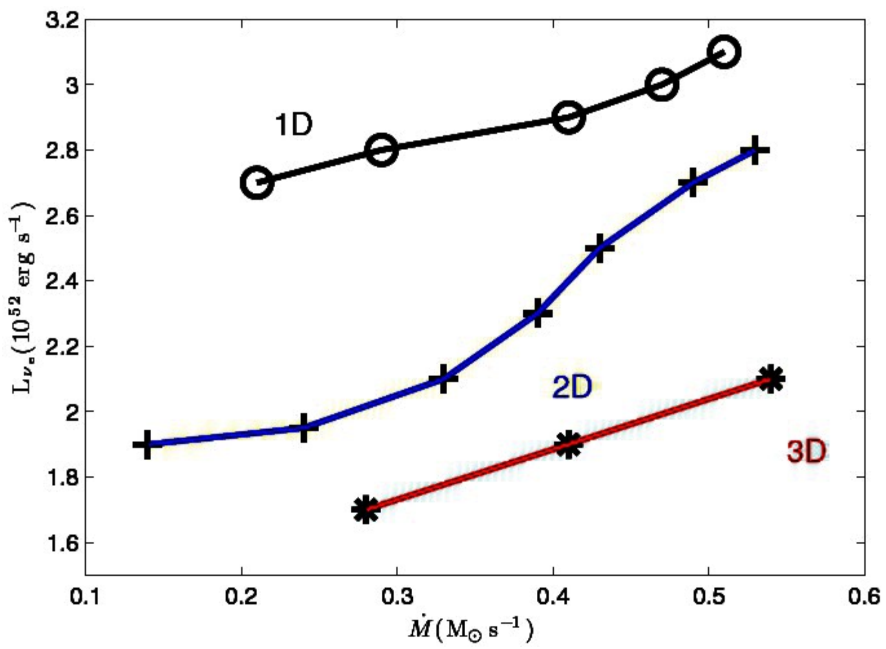

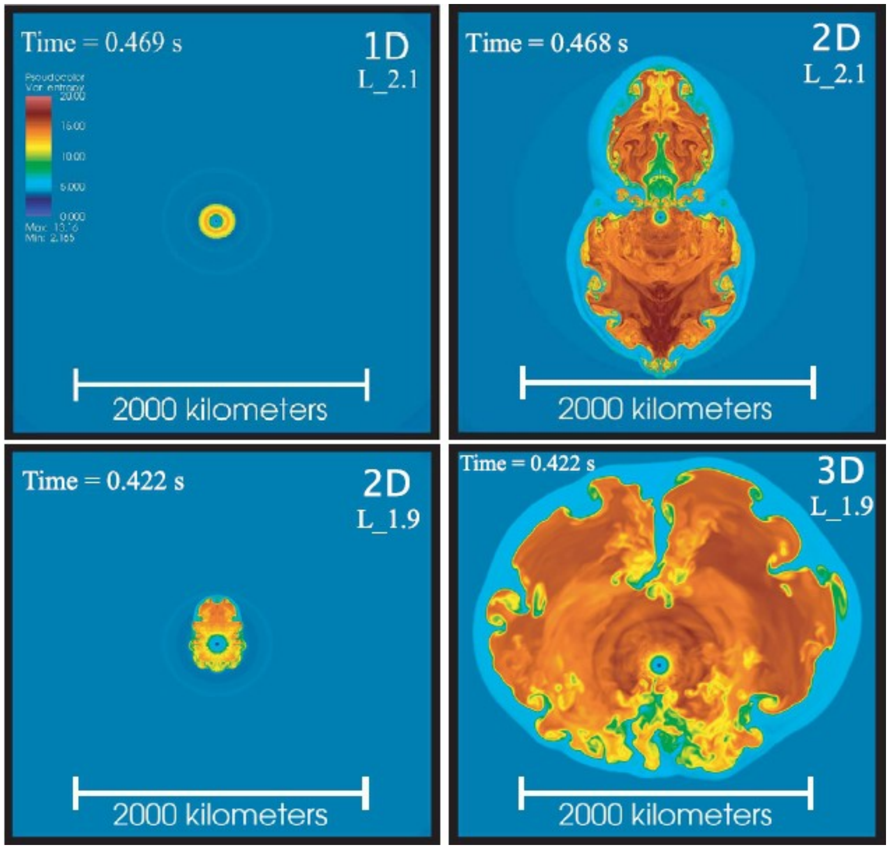

2D-3D Differences in Parametric Explosion Models

- F. Hanke (Diploma Thesis, MPA, 2010) in agreement with L. Scheck (PhD Thesis, MPA, 2007) could not confirm the findings by Nordhaus et al. (2010) ! 2D and 3D simulations for 11.2 M_{sun} and 15 M_{sun} progenitors are very similar but results depend on numerical grid resolution: 2D with higher resolution explodes easier, 3D shows opposite trend!

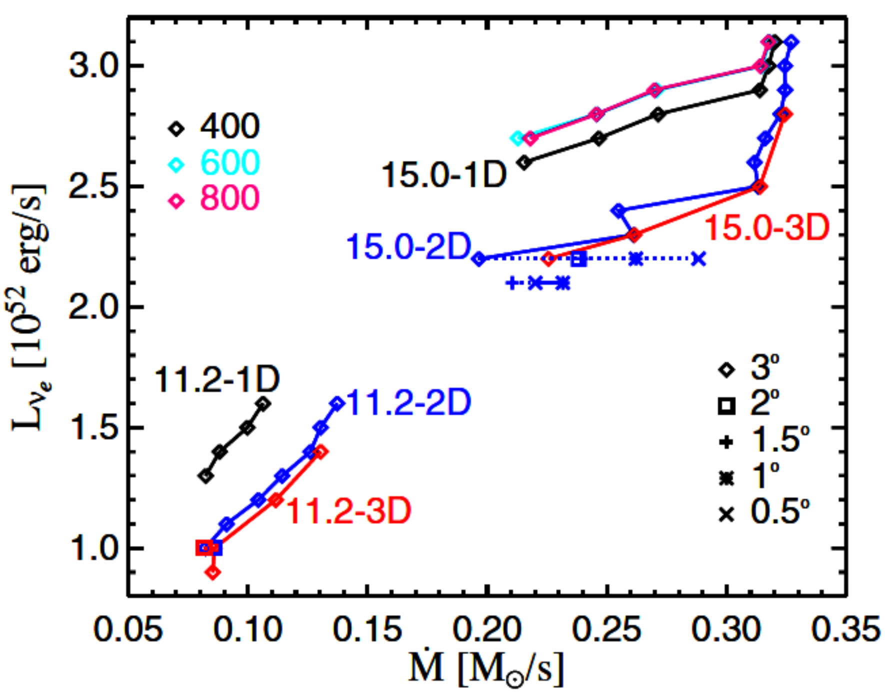

Hanke et al., ApJ 755 (2012) 138, arXiv:1108.4355

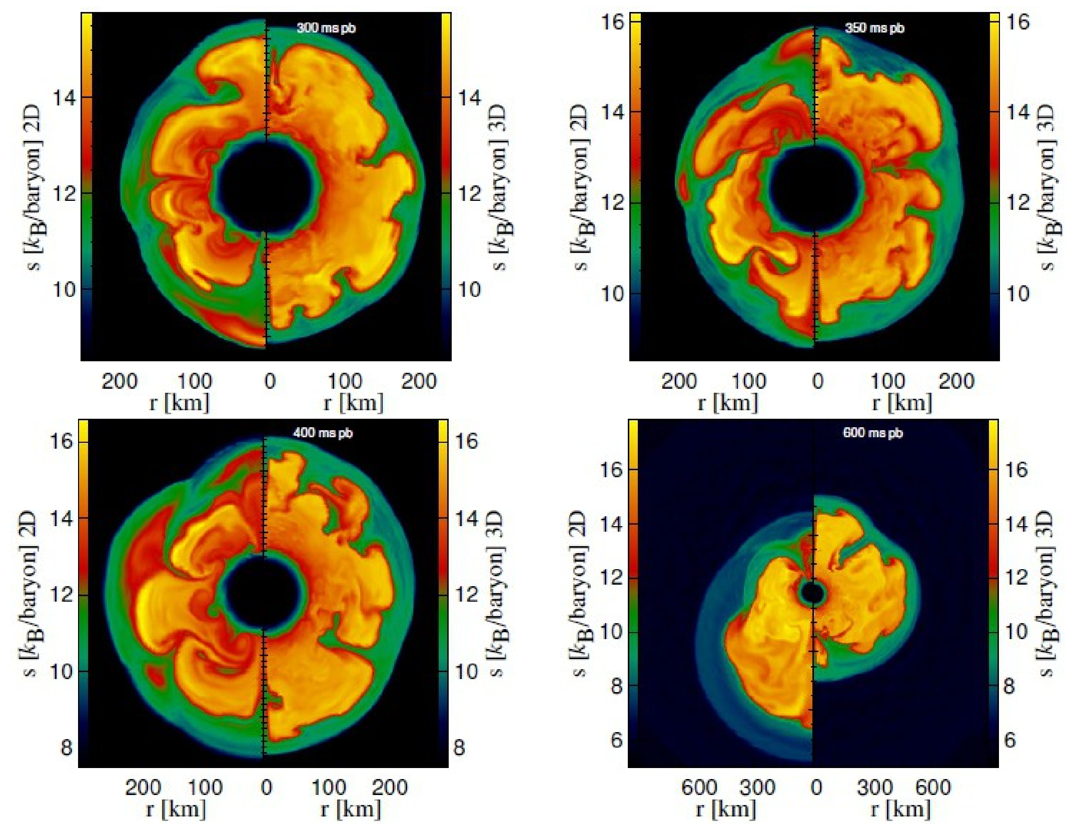

2D & 3D slices for 11.2 M_{sun} model, L = 1.0*10^{52} erg/s

Growing "Diversity" of 3D Results

- Dolence et al. (arXiv:1210.5241) find much smaller 2D/3D difference of critical luminosity, but still slightly earlier explosion in 3D.
- Takiwaki et al. (ApJ 749:98, 2012) obtain explosion for an 11.2 M_{sun} progenitor in 3D later than in 2D. Find a bit faster 3D explosion with higher resolution.
- Couch (arXiv:1212.0010) finds also later explosions in 3D than in 2D and higher critical luminosity in 3D!
  But critical luminosity increases in 2D with better resolution.
- Ott et al. (arXiv:1210.6674) reject relevance of SASI in 3D and conclude that neutrino-driven convection dominates evolution.

Reasons for 2D/3D differences and different results by different groups are not understood!

Growing "Diversity" of 3D Results

- These results do not yield a clear picture of 3D effects.

  But:

- The simulations were performed with different grids (cartesian+AMR, polar), different codes (CASTRO, ZEUS, FLASH, Cactus, Prometheus), and different treatments of input physics for EOS and neutrinos, some with simplified, not fully self-consistent set-ups.
- Resolution differences are difficult to assess and are likely to strongly depend on spatial region and coordinate direction.
- Partially compensating effects of opposite influence might be responsible for the seemingly conflicting results.
- Convergence tests with much higher resolution and detailed code comparisons for "clean", well defined problems are urgently needed, but both will be ambitious!

Full-Scale 3D Core-Collapse Supernova Models with Detailed Neutrino Transport

3D Supernova Models

PRACE grant of 146.7 million core hours allows us to do the first 3D simulations on 16.000 cores.

TGCC Curie

SuperMUC Petascale System

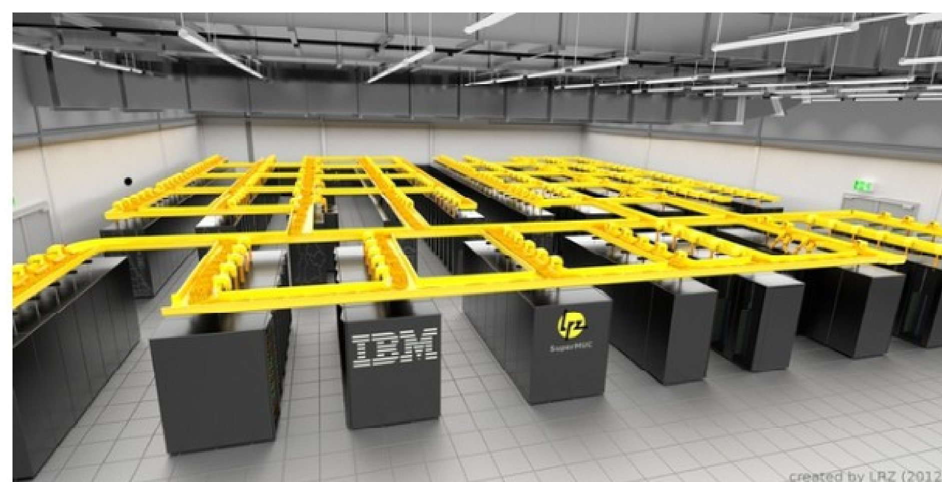

Computing Requirements for 2D & 3D Supernova Modeling

Time-dependent simulations: t ~ 1 second, ~ 10^6 time steps!

CPU-time requirements for one model run:

- **In 2D with 600 radial zones, 1 degree lateral resolution:**

  ~ $3 \cdot 10^{18}$ Flops, need ~10^6 processor-core hours.

- **In 3D with 600 radial zones, 1.5 degrees angular resolution:**

  ~ $3 \cdot 10^{20}$ Flops, need ~10^8 processor-core hours.

PRACE Partnership for Advanced Computing in Europe

NIC John von Neumann Institut für Computing

HLRS

rzg IPP Rechen-Zentrum Garching

Leibniz-Rechenzentrum der Bayerischen Akademie der Wissenschaften

3D Core-Collapse Models

11.2 M_{sun} progenitor

(Janka et al., PTEP 2012)

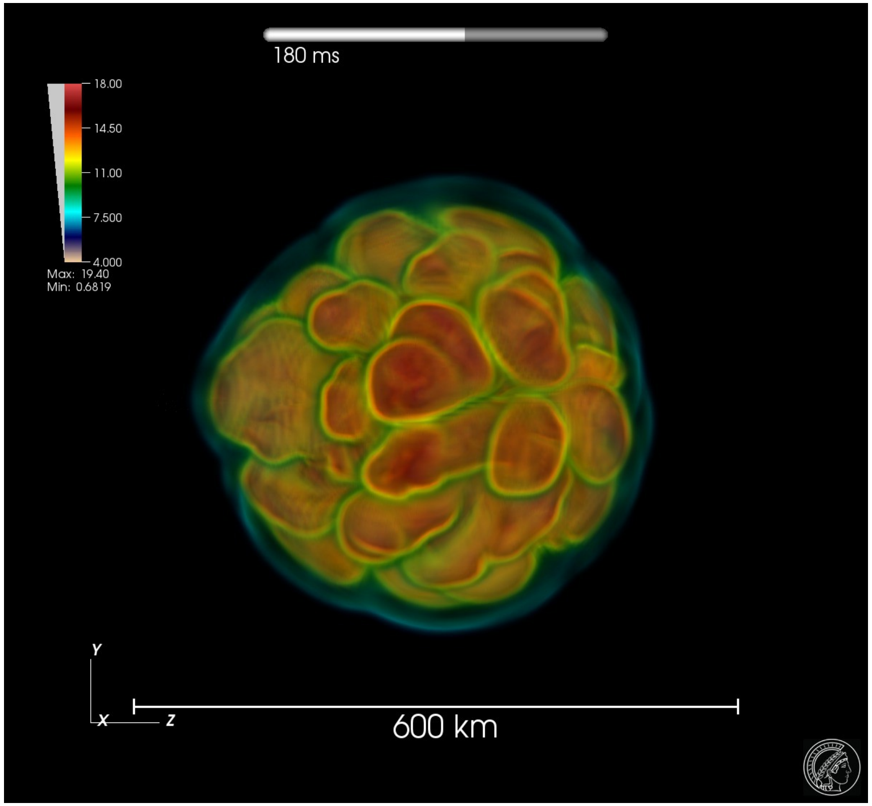

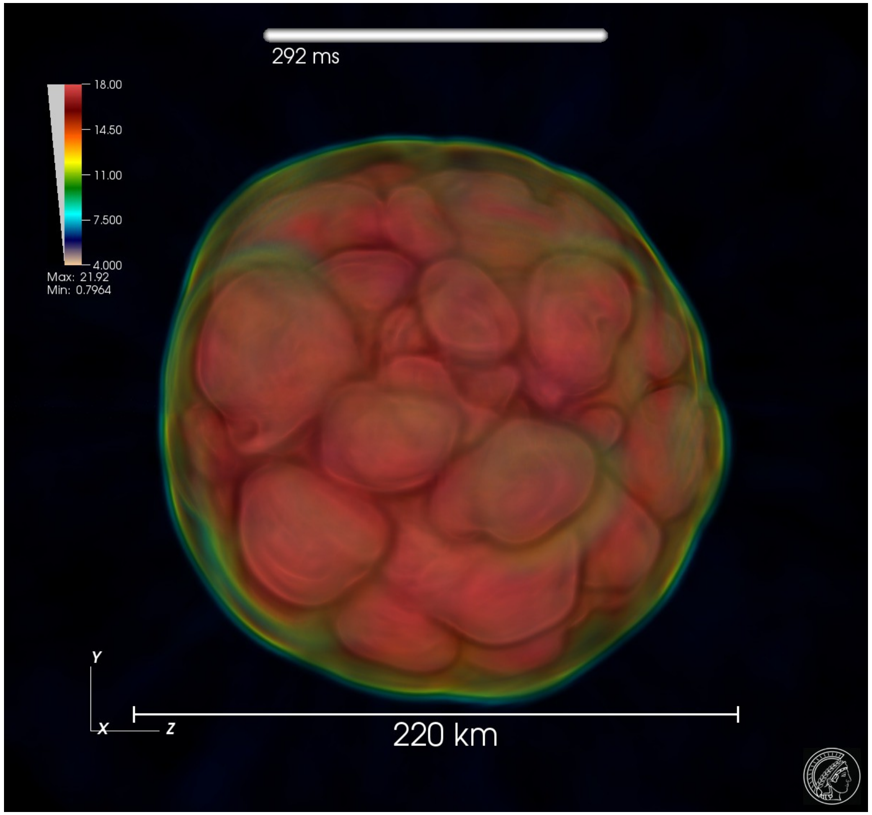

Florian Hanke, PhD project

3D Core-Collapse Models

27 M_{sun} progenitor

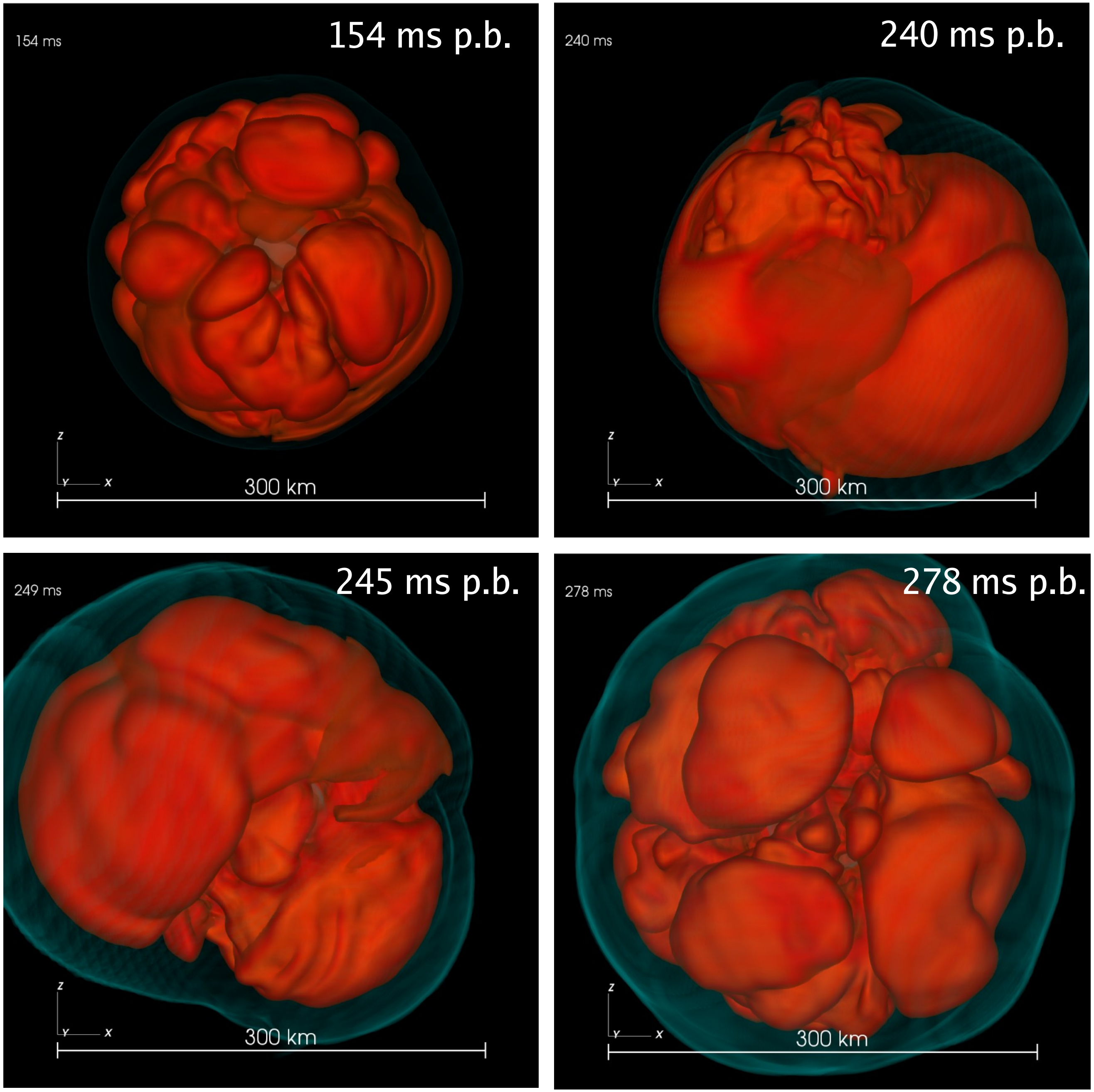

Florian Hanke,
PhD project

Laboratory Astrophysics

"SWASI" Instability as an analogue of SASI in the supernova core

Foglizzo et al., PRL 108 (2012) 051103

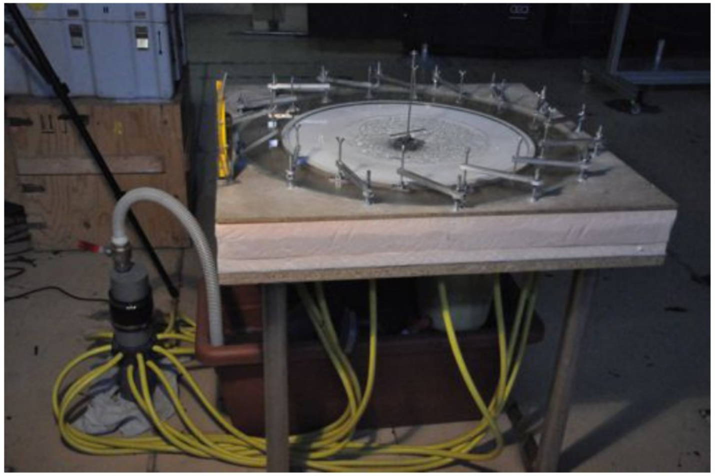

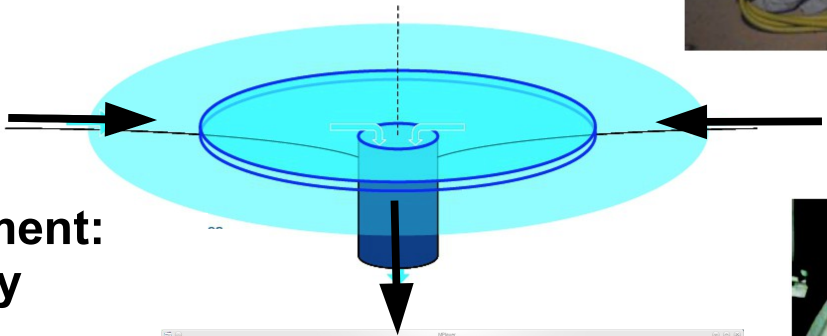

Constraint of experiment:
No convective activity

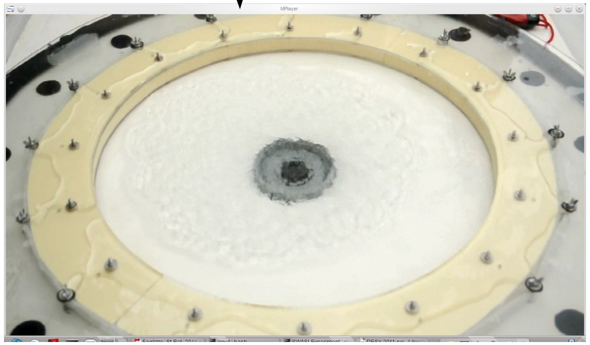

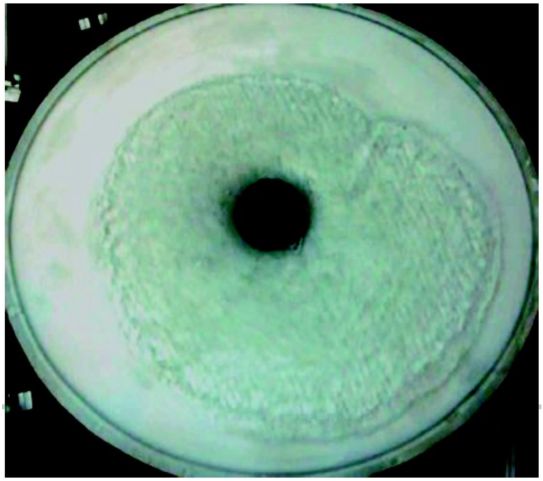

Numerical Convergence?

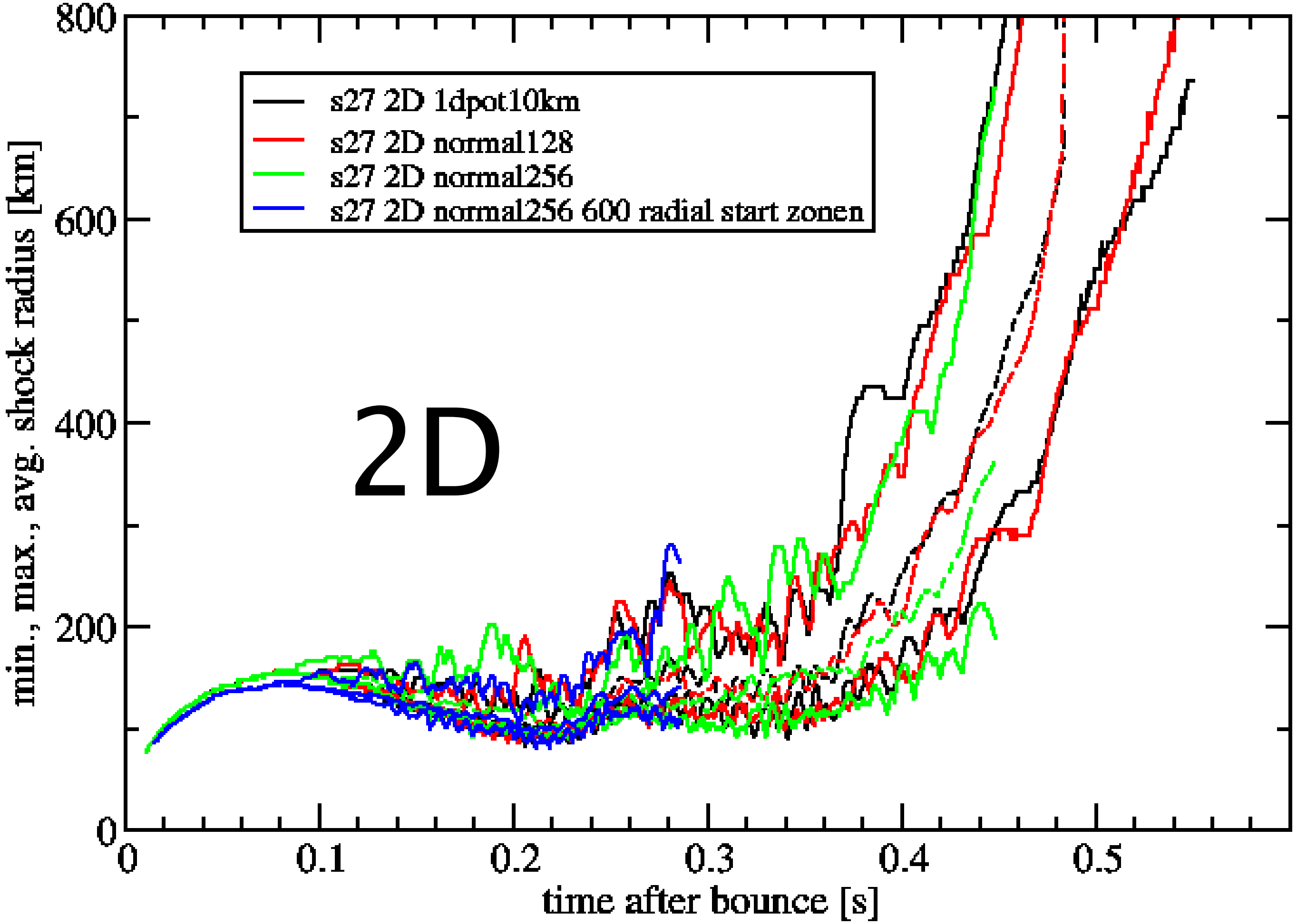

Florian Hanke, PhD project

2D simulations are converged; no difference between 0.7, 1.4, and 2.04 degrees angular resolution.

But: 3D simulations may need more resolution for convergence than in 2D!

Numerical Convergence?

Hanke et al., ApJ 755 (2012) 138; arXiv:1108.4355

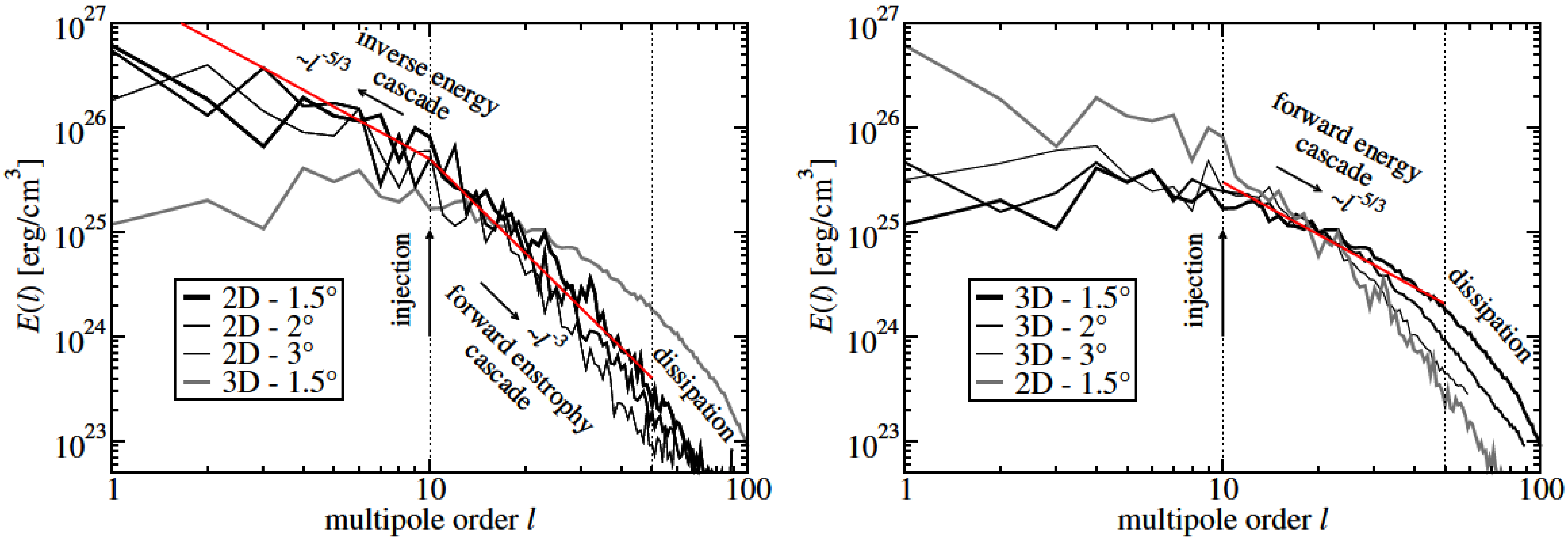

Figure 16. Turbulent energy spectra $E(l)$ as functions of the multipole order l for different angular resolution. The spectra are based on a decomposition of the azimuthal velocity v_θ into spherical harmonics at radius $r = 150$ km and 400 ms post-bounce time for 15 $M_\odot$ runs with an electron–neutrino luminosity of $L_{\nu_e} = 2.2 \times 10^{52}$ erg s^{-1}. Left: 2D models with different angular resolution (black, different thickness) and, for comparison, the 3D model with the highest employed angular resolution (gray). Right: 3D models with different angular resolution and, for comparison, the 2D model with the highest employed angular resolution (gray). The power-law dependence and direction of the energy and enstrophy cascades (see the text) are indicated by red lines and labels for 2D models in the left panel and 3D models in the right panel. The left vertical, dotted line roughly marks the energy-injection scale, and the right vertical, dotted line denotes the onset of dissipation at high l for the best-displayed resolution.

Turbulent energy cascade in 2D from small to large scales, in 3D from large to small scales!   =====>   **More than 2 degree resolution needed in 3D!**

Summary

- Modelling of SN explosion mechanism has made considerable progress.
- 2D relativistic models yield explosions for "soft" EoSs. Explosion energy tends to be on low side (except recent models by Bruenn et al., arXiv:1212.1747).
- 3D modeling has only begun. No clear picture of 3D effects yet. **But SASI can dominate (certain phases) also in 3D models!**
- 3D SN modeling is extremely challenging and variety of approaches for neutrino transport and hydrodynamics/grid choices will be and need to be used.
- Numerical effects (and artifacts) and resolution dependencies in 2D and 3D models must still be understood.
- Bigger computations on faster computers are indispensable, but high complexity of highly-coupled multi-component problem will demand special care and quality control.

For concise reviews of most of what I will say, see

ARNPS 62 (2012) 407, arXiv:1206.2503
and
PTEP 2012, 01A309, arXiv:1211.1378

REVIEWS IN ADVANCE

Explosion Mechanisms of Core-Collapse Supernovae

Hans-Thomas Janka

Max Planck Institute for Astrophysics, D-85748 Garching, Germany;
email: thj@mpa-garching.mpg.de